https://doi.org/10.32604/zkg.2026.077973

REVIEW

Sustainable and rapid-hardening alkali-activated materials for pavement repair: a systematic review of performance and maturity-based prediction

Muhamad Aditya Pratama[1], Stefanus Adi Kristiawan[2,*] and Florentina Pungky Pramesti[2]
[1]Master Program in Civil Engineering, Faculty of Engineering, Sebelas Maret University, Surakarta, Indonesia
[2]Civil Engineering Department, Faculty of Engineering, Sebelas Maret University, Surakarta, Indonesia
*Corresponding Author: Stefanus Adi Kristiawan. Email: s.a.kristiawan@ft.uns.ac.id

Received: 21 December 2025; Accepted: 25 May 2026

ABSTRACT: Rapid-repair of concrete pavements is crucial for minimizing traffic disruptions and restoring serviceability in time-crucial situations. While Portland-based and alternative rapid-hardening binders are frequently used, these materials often trade off between cost, durability, and environmental concerns. This systematic review explores the potential of AAMs as a sustainable alternative for rapid pavement repair, with particular emphasis on early-age performance and the reliability of maturity methods for non-destructive strength monitoring. Adhering to PRISMA guidelines, this study screened the published literature from 2000 to 2025 using PICO(S) criteria, focusing on AAM interventions for rapid pavement repair and comparing them with conventional and alternative binders where applicable. The review correlates precursor-activator systems with early mechanical performance and assesses the applicability of maturity-based approaches for predicting *in-situ* strength development. The findings indicate that optimized slag-containing AAMs achieved compressive strengths of about 16–28 MPa within 6–8 h, offering superior bonding and durability. Additionally, maturity methods demonstrate strong potential for real-time strength prediction; however, their distinct and complex non-linear reaction kinetics necessitate the rigorous, system-specific recalibration of key thermodynamic parameters. Despite these advantages, persistent challenges remain, including high sensitivity to activator chemistry and curing conditions, poor volumetric stability, supply chain and economic uncertainties, and a critical lack of standardized testing and long-term field data. This review affirms that integrating optimized AAM formulations with maturity-based prediction tools provides a high-performance, low-carbon pathway for accelerating repair operations. To support reliable performance-based decisions for early traffic reopening, future research should adopt a multi-scale, lifecycle-oriented framework that connects materials design, structural performance, and long-term field validation.

KEYWORDS: Alkali-activated material; concrete pavement repair; early-age strength; maturity method; sustainable repair material

1 Introduction

Concrete pavements form the structural backbone of modern transportation networks, playing an indispensable role in supporting economic productivity and ensuring the efficient movement of goods and people. Their superior load-bearing capacity, long service life, and resilience under repetitive traffic loading and harsh environmental conditions make them a preferred choice for critical infrastructure such as highways, airports, and industrial facilities [1]. However, despite their robust design, concrete pavements are not immune to deterioration. Repeated mechanical stresses, freeze–thaw cycles, and exposure to aggressive agents such as chlorides and de-icing salts progressively lead to distresses including cracking, spalling, scaling, and joint failures, all of which compromise pavement performance and increase maintenance demands [1–4]. These cumulative degradations not only reduce structural integrity but also impose major economic burdens [5], as reflected by the USD 1.6 trillion projected for pavement and bridge repair in the United States between 2020 and 2025 [4], and similarly in the United Kingdom where deferred highway maintenance is estimated to cost £90 billion by 2026 [6]. Furthermore, the associated service interruptions, traffic delays, and energy losses translate into elevated user costs and productivity losses,

MATERIALS

emphasizing the critical need for repair materials and strategies that deliver rapid strength gain, durability, and sustainability.

In selecting suitable repair materials, engineers must carefully consider the correlation between the type of distress, pavement structure, and the expected performance characteristics of the repair material. For instance, partial-depth repairs may suffice for surface cracking on scaling, whereas full-depth restoration is required for severe joint or structural damage [1]. The selected material must achieve sufficient bond strength with existing substrate, maintain dimensional stability, and exhibit adequate resistance to thermal and mechanical stresses [3, 7, 8]. However, conventional repair materials often fall short of expectations, particularly under high-traffic and variable climate conditions.

Portland-based binders remain the dominant choice for pavement repair due to their availability and familiarity in construction practice. Yet, they are hindered by several intrinsic limitations. First, conventional Portland-based mixtures exhibit relatively slow hydration kinetics, delaying early strength development and prolonging roadway closures [9]. This limitation significantly affects high-volume roads where even short-term closures can cause substantial economic disruption [3, 10]. Second, Ordinary Portland Cement (OPC) is a major contributor to global carbon emissions, responsible for approximately 7–8% of total CO_2 output due to the calcination of limestone and the energy-intensive nature of clinker production [11, 12]. Third, Portland-based repair mortars can display poor durability when exposed to freeze-thaw cycles, chloride ingress, and sulfate attack, leading to premature failure [13]. Furthermore, shrinkage remains a critical issue in conventional binders; while shrinkage of Portland-based is primarily driven by water evaporation and hydration, it often requires extensive mitigation strategies to prevent cracking that compromises long-term structural reliability [12].

Alternative rapid-hardening binders, including Calcium Aluminate Cement (CAC), Calcium Sulfoaluminate (CSA), and Magnesium Phosphate Cement (MPC), have been developed to address the issue of delayed strength gain [1, 14]. While these materials offer accelerated setting and high early strength, they are not without drawbacks. Their production remains energy-intensive, their raw materials are often costly or regionally limited, and they may experience durability challenges or incompatibility with OPC-based substrates under aggressive environments. Additionally, commercial polymer-modified mortars, while effective, can be prohibitively expensive [15]. These shortcomings create a pressing demand for sustainable, high-performance alternatives that balance early strength, long-term durability, and environmental responsibility.

The evolution of pavement maintenance increasingly emphasizes rapid-repair technologies that minimize downtime and reduce user delays. Rapid-hardening materials are engineered to develop sufficient early-age strength, often within 4 to 24 h, to allow traffic to reopen sooner than conventional systems [5, 10]. To fully leverage these materials, predictive tools such as the maturity method have been adopted. This non-destructive technique estimates *in-situ* strength development by monitoring the material's specific temperature-time history. The rationale for incorporating the maturity method in pavement repair is two-fold: it ensures structural safety by preventing premature opening to traffic, while simultaneously eliminating unnecessary lane closures caused by conservative, fixed-time waiting periods [5, 16, 17]. Consequently, this method transforms maintenance from a prescriptive process into a performance-based one.

Despite such progress, the sustainability and environmental performance of rapid-repair materials remains a concern. OPC-based binders and many alternative formulations still exhibit high embodied carbon and limited recyclability. Hence, the next frontier in pavement repair lies in developing binders that are not only rapid-hardening but also low-carbon and resource-efficient.

To address these challenges, Alkali-Activated Materials (AAMs), including the sub-class of lower-calcium systems which are also known as "geopolymers" [18, 19], have emerged as promising alternatives to conventional cementitious binders. AAMs are synthesized by activating aluminosilicate precursors such as Ground Granulated Blast Furnace Slag (GGBFS, herein after referred to as slag), fly ash, or metakaolin using alkaline solutions. Depending on the precursors and activators used, the reaction forms a dense binder of Sodium-, Potassium-, or Calcium-Alumino-Silicate Hydrate (N/K/C-A-S-H), establishing a complex structural framework that ensures excellent mechanical and durability properties [19–23]. Some of these systems are capable of achieving rapid setting and high-early strength [8, 24, 25], making them particularly suitable for pavement repair applications where minimal cover time is critical. Notable advancements in regulatory recognition, such as the publication of the ASTM C1948 standard for Alkali-Activated Cementitious Materials, have further paved the way for broader industrial adoption and standardized testing of these systems [12].

A growing body of research has confirmed that the suitability of AAMs for structural and repair applications, with Pavel et al. [8] demonstrating early compressive strengths exceeding 35 MPa within 24 h in slag-based AAM concretes, and Addellatief et al. [22] reporting up to 134 MPa in Ultra-High Performance Geopolymer Concrete (UHPGC) under heat curing; even under ambient conditions, ultra-fine slag-based AAM mortars have been shown to achieve approximately 60% of their strength for 28 days in 1 day [26], supporting rapid-repair potential. Structural

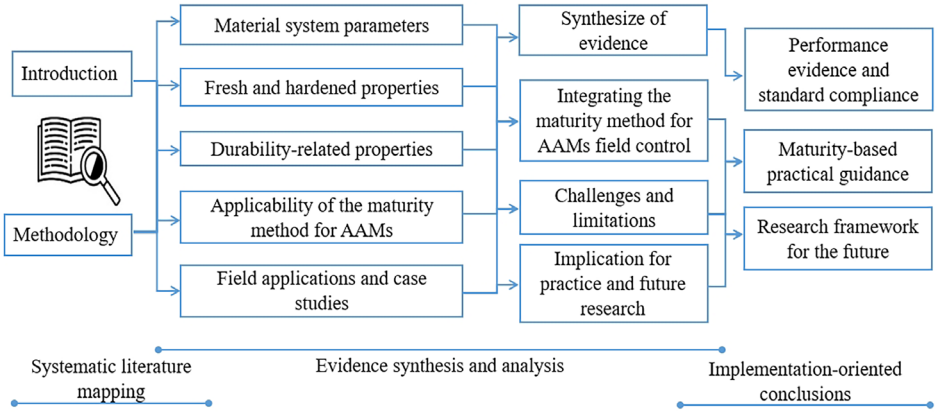

Figure 1 Conceptual framework illustrating the analytical structure of the review, linking systematic literature mapping and evidence synthesis to implementation-oriented insights

rehabilitation studies further confirmed superior performance, as reinforced beam repaired with slag-based AAM mortars exhibited higher load-carrying capacity and bond strength than OPC-based [7], in line with findings by Magee et al. [6] and Chen et al. [27] that metakaolin-slag AAM mortars provide excellent wear resistance, skid durability, and adhesion to aged concrete surfaces. Beyond mechanical advantages, AAMs also provides substantial environmental benefits, with CO_2 emissions up to four times lower than OPC, ranging between 41 and 261 kg CO_2-eq/m^3 [11], as reflected in practice through projects such as Brisbane West Wellcamp Airport, where hybrid AAM concrete achieved an 80% reduction in CO_2 emissions [28]. Cost efficiency is also improved, as the use of waste-derived precursors such as fly ash and slag lowers productions costs while promoting circular resource utilization [9,15], and recent innovations in hybrid systems incorporating limited OPC and polymer modification have further enhanced adhesion at the repair interface and resistance to acid and sulfate exposure, thereby extending service life in pavement applications [15].

Despite growing evidence of the mechanical, durability, and environmental benefits of AAMs, their adoption in pavement repair remains limited. The current body of research is fragmented, with studies varying widely in precursor composition, activator concentration, curing conditions, and testing methodologies [29]. Additionally, specific challenges such as shrinkage behavior, which can be more pronounced in AAMs compared to OPC due to high mesopore volume and capillary stress, require careful mitigation through precise mix design and curing protocols [12]. In particular, maturity-based strength prediction methods require rigorous reassessment; the distinct reaction kinetics and thermal sensitivity of AAMs relative to OPC, together with the absence of standardized non-destructive field monitoring techniques, significantly undermine the reliability of real-time strength estimation and delay the transition from laboratory research to safe pavement reopening in practice. As such, there is a lack of systematic synthesis that integrates these findings to assess the comprehensive potential of AAMs as sustainable and rapid-hardening repair materials.

Therefore, this systematic review addresses the fragmented understanding of AAMs in rapid pavement repair by integrating early-age performance, durability behavior, and predictive modeling within a unified analytical perspective. As illustrated in Figure 1, the review is structured through a conceptual framework that links literature mapping and evidence synthesis with implementation-oriented analysis. Specifically, the study seeks to examine material systems, including precursor-activator combinations and associated performance parameters; evaluate the applicability of predictive tools such as the maturity method for field-based strength monitoring; identify key technical challenges and limitations that may hinder practical adoption; and outline implications for engineering practice while highlighting directions for future research.

2 Methodology

The study employs a systematic review approach to comprehensively identify, evaluate, and synthesize existing research on the use of AAMs and/or geopolymers for the rapid repair of concrete pavements. The methodology adheres to Preferred Reporting Items for Systematic Review and Meta-Analyses (PRISMA) 2020 Statement [30] to ensure transparency, rigor, and reproducibility, consistent with earlier recommendations for minimizing bias in evidence synthesis [31]. The review process encompasses a detailed search strategy, predefined inclusion and exclusion criteria based on the PI-CO(S) framework, a structured multi-stage screening procedure, and systematic data extraction [32].

A rigorous and transparent search strategy was developed in accordance with established guidelines for evidence-based review [33, 34]. A search tool was used to systematically group and organize keywords based on the core concepts of the research aim [32]. The search targeted peer-reviewed literature indexed in Scopus and Google

Scholar, with Publish or Perish (PoP) software utilized to facilitate structured retrieval and reference management. A comprehensive Boolean query was formulated to integrate three conceptual domains: Material ("alkali-activated material" or "geopolymer"), Performance ("rapid-set" or "rapid-hardening" or "high-early strength"), and Application ("repair" or "pavement repair" or "maturity method"), combined using the operators "AND" and "OR" to ensure that only relevant studies addressing rapid-hardening AAMs for pavement repair were capture.

Study selection was conducted using a rigorous PICO(S) framework focused on concrete pavement repair (Population), using AAM (Intervention) as an alternative to conventional cementitious binders (Comparison). The screening prioritized studies reporting key performance metrics, including early-age strength, volumetric stability, and interfacial bond integrity (Outcome), and was limited to peer-reviewed experimental studies, reviews, and conference proceedings in English published from 2000 onward (Study type). As illustrated in Figure 2, the PRISMA flow diagram shows that 496 records were initially identified through database searches; after removing 226 duplicates, 270 records were screened based on titles and abstracts, resulting in the detailed eligibility assessment of 116 full-text articles. Ultimately, 94 studies met all inclusion criteria and were incorporated into the qualitative synthesis, forming the empirical basis of this systematic review.

Subsequent to the selection process, eligible studies were systematically compiled and reviewed for qualitative synthesis. Key information related to material system parameters, fresh- and hardened-state properties, durability, maturity methods, and field applications was extracted and critically analyzed to identify the main factors controlling the performance of rapid-hardening AAMs for repair applications.

3 Factors controlling the performance of rapid-hardening AAMs

The performance of rapid-hardening AAMs is governed by the interaction between precursor chemistry and activator configuration. This section discusses the key factors controlling fresh properties, early-age strength, and durability performance, with particular emphasis on their influence on dissolution kinetics, gel formation, and engineering behavior. The applicability of maturity-based prediction methods is also evaluated as a tool for field-based strength monitoring and supporting repair strategies.

3.1 Material system parameters

3.1.1 Precursors

Precursor chemistry is the primary factor controlling reaction kinetics, gel stoichiometry, and the resulting engineering performance of AAM systems. In rapid pavement repair applications, the balance between the CaO/SiO_2 and SiO_2/Al_2O_3 ratios determines the dominant reaction pathway by regulating the availability of reactive calcium, silicate, and aluminate species. These oxide ratios represent the overall precursor composition, while molar ratios such as Ca/Si and Si/Al describe the stoichiometry of the resulting gel phases. Class

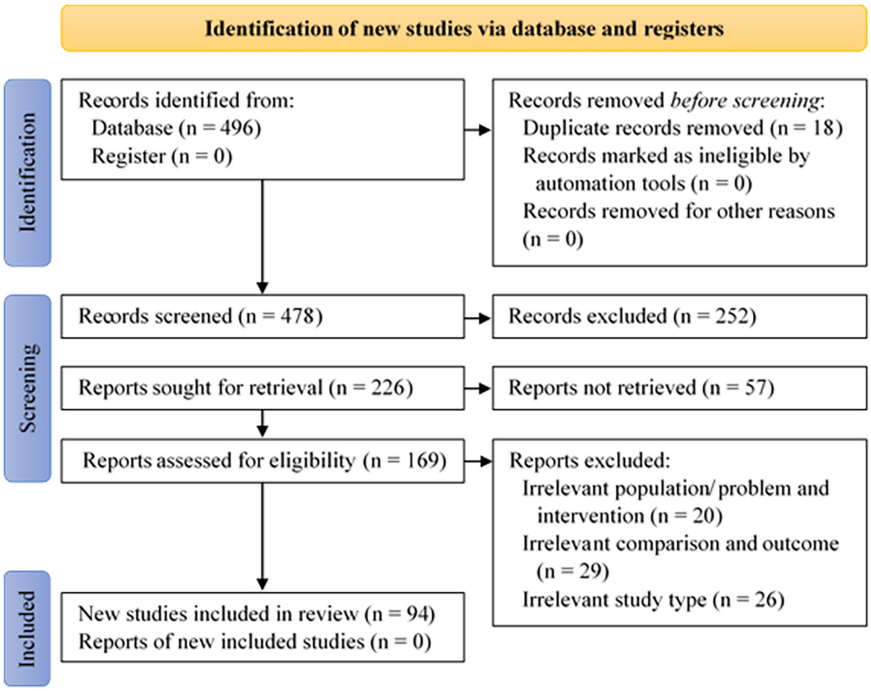

Figure 2 PRISMA 2020 flow diagram illustrating the study identification, screening, eligibility, and inclusion process

F fly ash and metakaolin typically exhibit CaO/SiO_2 ratios below 0.3 and higher SiO_2/Al_2O_3 ratios (2–3), favoring the gradual formation of N-A-S-H (or K-A-S-H) gels. In contrast, slag and Class C fly ash generally show CaO/SiO_2 ratios above 0.8 and lower SiO_2/Al_2O_3 ratios (1–2), promoting rapid precipitation of C-(A)-S-H gels. Hybrid systems combining slag with Class F fly ash or metakaolin typically fall within intermediate CaO/SiO_2 ratios (0.4–0.8) and moderate SiO_2/Al_2O_3 ratios (2–3), enabling the formation of cross-linked (N,C)-A-S-H networks. As summarized in Table 1, these different chemical regimes lead to distinct microstructural evolution pathways and engineering performance across different AAM systems.

In low-calcium systems, alkaline activation of Class F fly ash follows a destruction-polycondensation mechanism in which the high bond energy of Si-O-Si and Si-O-Al linkages limits dissolution at ambient temperature [23]. Once dissolved, silicate and aluminate monomers are released and subsequently polycondense, with Na^+ (or K^+) ions from the activator balancing the negative charge of $[AlO_4]^-$ tetrahedra within the framework to form a stable N-A-S-H (or K-A-S-H) gel network [21, 23, 35]. However, early precipitation of aluminum species can create a passivation layer on Class F fly ash particles, inducing a dormant period that delays gel densification and results in a porous capillary structure at early ages [23, 35]. Mechanically, this leads to prolong setting times and insufficient early-age strength, making pure low-calcium systems unsuitable for rapid pavement repair where reopening is required within hours. Additionally, because N-A-S-H (or K-A-S-H) gels bind water less effectively than high-calcium systems, excess free water remains in capillary pores, increasing susceptibility to drying shrinkage upon evaporation [12, 36]. Metakaolin serves as an alternative high-purity, low-CaO precursor, a calcined and highly amorphous aluminosilicate, offers higher and more uniform reactivity at ambient temperature and can rapidly form stable N-A-S-H (or K-A-S-H) networks [37, 38], but its plate-like morphology increases water demand and may reduce workability or promote brittleness if not properly optimized.

Conversely, CaO-rich precursors such as slag (30–45% CaO) exhibit exceptional early-age strength due to their rapid alkaline activation. The reaction involves fast dissolution of the Ca-O-Si and Mg-O-Si network, accompanied by a sharp exothermic peak and the release of Ca^{2+} and silicate species, followed by rapid precipitation of disordered C-S-H, which subsequently incorporates aluminate species and charge-balancing Na^+ to form cross-linked C-(A)-S-H gels [23, 39, 40]. These C-(A)-S-H gels possess high space-filling capacity, rapidly refining the pore structure into a dense mesoporous network, which underpins the superior early mechanical performance of slag-based AAMs [26, 41]. However, this advantage is offset by a pronounced durability risk: rapid gel formation induces severe self-desiccation within the refined mesopores, generating high capillary stresses that lead to significant autogenous and plastic shrinkage [42–44]. In thin pavement repair layers, these stresses often exceed the immature tensile strength, promoting microcracking and premature debonding at the interfacial transition zone (ITZ). Class C fly ash, with higher inherent CaO content (typically >18%) than Class F fly ash, represents another option, enabling the coexistence of C-(A)-S-H and N-A-S-H gels. While elevated-temperature curing can yield very rapid strength development (e.g., >90% of 28 days strength within 24 h at 70°C) [45], variations in calcium content strongly affect rheology and mechanical response, necessitating strict material characterization. Under ambient curing conditions typical of rapid pavement repair, Class C fly ash-based AAMs often still require additional calcium sources or highly concentrated activators to achieve sufficiently early-age strength.

To reconcile the trade-off between early strength and volumetric stability, hybrid precursor systems utilize the synergistic coexistence of C-(A)-S-H and N-A-S-H gels, where the incorporation of Class F fly ash or metakaolin into slag-based matrices modifies microstructural evolution. Such hybrid systems are widely recognized as an effective strategy for rapid pavement repair because precursor chemistry governs both reaction kinetics and field performance, requiring a balanced combination of CaO-rich and aluminosilicate source precursors. Unlike purely high-calcium systems, which may exhibit rapid reactions and significant autogenous shrinkage, the inclusion of low-CaO precursors rich in amorphous SiO_2 and Al_2O_3 moderate dissolution kinetics and stabilizes gel development. In particular, slag-Class F fly ash blends activated with NaOH and Na_2SiO_3 follow a staggered, multi-stage reaction pathway that enables early-age strength gain for traffic reopening while maintaining long-term durability.

The reaction is initiated by the alkaline dissolution of amorphous phases, releasing Si^{4+}, Al^{3+}, and Ca^{2+} ions into the pore solution [23]. Slag dissolves more rapidly than Class F fly ash because breaking Ca-O-Si, Mg-O-Si, and Al-O-Al bonds requires less energy than disrupting the more stable Al-O-Si bonds in Class F fly ash-based systems [23, 46]. The high availability of Ca^{2+} promotes the rapid precipitation of disordered C-(A)-S-H gels, which form the primary structural skeleton responsible for early-age strength and enable early traffic reopening [23, 47]. During this stage, partially reacted or unreacted Class F fly ash particles act as nucleation sites that further accelerate C-(A)-S-H formation [23, 48]. As curing progresses, the delayed dissolution of Class F fly ash activates polycondensation reactions that generate a three-dimensional N-A-S-H framework, progressively filling capillary pores and densifying the matrix [13, 23]. Importantly, C-(A)-S-H

Table 1 **Comparison of gel formation mechanisms and associated engineering performance in different AAM systems [23, 35, 37, 38, 45–48, 50]**

Feature	Low-calcium systems	High-calcium systems	Hybrid (binary) systems
Primary precursors	Class F fly ash, metakaolin	Slag, Class C fly ash	Slag + Class F fly ash/metakaolin
Dominant gel phase	K/N-A-S-H (Potassium- or Sodium-alumino-silicate hydrate)	C-(A)-S-H (Calcium-(alumino)-silicate hydrate)	(N,C)-A-S-H (Hybrid cross-linked network)
Primary bond breaking	High energy required to break stable Si-O-Si and Al-O-Si bonds.	Dissolution of the disordered Ca-Si-O and Mg-O-Si network.	Multi-stage: Rapid dissolution of Ca-bonds followed by Al-Si oligomer release.
Structural Role of Cations	Na^+ (or K^+) acts as a charge balancer within the $[AlO4]^-$ tetrahedral network.	Ca^{2+} acts as a network former/modifier, creating a chain-like structure.	Ca^{2+} ions progressively substitute into the N-A-S-H framework, increasing cross-linking.
Reaction kinetics	Slow/Insufficient: Limited reactivity at ambient temp; often requires heat curing.	Rapid/Aggressive: Intense early-age reactivity and fast setting times.	Regulated: Staggered dissolution provides a "controlled" reaction window.
Microstructural evolution	Coarser pore structure with higher levels of free water.	Highly refined mesoporous network; very high capillary tension.	Bimodal distribution: Early C-(A)-S-H skeleton refined by later N-A-S-H "filling."
Early-age strength	Low; unsuitable for rapid traffic reopening.	Exceptional: Achieves high structural capacity within hours.	Optimal: Balanced early strength development with continued gain.
Dimensional stability	Low risk of autogenous shrinkage but high drying shrinkage risk.	Poor: Intense self-desiccation leads to high autogenous shrinkage and ITZ debonding.	Excellent: "Dilution" of calcium content reduces capillary tension and mitigates cracking.

and N-A-S-H do not evolve independently; chemical restructuring occurs as Ca^{2+} partially substitutes Na^+ within the aluminosilicate network to form cross-linked (N,C)-A-S-H phases, while additional aluminum incorporation into C-(A)-S-H bridging sites enhances structural connectivity [13, 23]. The macroscopic performance of the repair system therefore reflects the balance between these reaction pathways: slag-rich processes favor rapid-hardening but increase shrinkage risk, whereas Class F fly ash incorporation refines the pore structure, improves gel-aggregate bonding, and promotes a more homogeneous and thermodynamically stable microstructure.

Beyond binary blends, several studies have extended precursor design toward ternary systems [22, 49–51], aiming to further tailor reaction kinetics and microstructural evolution specifically for pavement applications. The incorporation of silica fume into slag-Class F fly ash matrices has been reported to improve particle packing and early-age strength more effectively than metakaolin in certain ternary configurations [49]. Its ultrafine particles supply highly reactive amorphous silica that refines capillary pores, reduces permeability, and enhances resistance to de-icing salts and freeze thaw cycles [22]. Other investigations introduced supplementary materials such as red mud [52], flue gas desulfurization gypsum [52], and municipal solid waste incineration fly ash [53] to promote co-precipitation of cross linked gels and accelerate setting, in some cases achieving very rapid strength development suitable for emergency repair scenarios. However, these performance gains are highly formulation dependent. As evidenced by the strength reduction observed when CaO-rich parawood ash was incorporated into low-silicate activator systems [54] and by the sensitivity of gel stability to activator composition [55], chemical compatibility between precursors and alkaline activators remains a decisive yet insufficiently systematized factor.

3.1.2 Alkaline activators

The alkali activation mechanism is a critical determinant of reaction kinetics, gel chemistry, and constructability of AAM systems. Alkaline activators typically consist of alkali anions (OH^-, SiO_3^{2-}, CO_3^{2-}) combined with alkali or alkaline-earth cations (Na^+, K^+, Ca^{2+}) [23], and variations in activator chemistry directly influence reaction pathways and resulting mechanical performance. Among available options, sodium (Na-based) systems dominate pavement repair applications due to superior cost-effectiveness and commercial availability compared with potassium (K-based) alternatives, despite the latter's potential advantages in reduced viscosity and efflorescence [4, 22, 23, 56]. Accordingly, most studies employ conventional two-part systems composed of NaOH, either alone or combined with Na_2SiO_3 [27, 37, 40, 50, 57–62]. Na-based activation also demonstrates compatibility with calcium-rich mixtures that promote the formation of cross-linked (N,C)-A-S-H phases, as mentioned in Section 3.2.1, which is favorable for rapid strength development as well as long-term durability.

NaOH primarily establishes the high-pH environment required for the dissolution of aluminosilicate precursors, whereas Na_2SiO_3 contributes both alkalinity and soluble silica species; their combined use is more effective in enhancing

compressive strength than either component alone because NaOH adjusts the SiO_2/Na_2O ratio [50], which is defined as the silicate modulus (Ms) of the activator solution, thereby creating a chemically favorable reaction environment. Commercial Na_2SiO_3 solutions typically exhibit Ms values between 1.6 and 3.85; however, excessively high Ms can impair silicate solubility, trigger premature polymerization, increase viscosity, and hinder uniform mixing, while excessively low Ms accelerates dissolution and setting but may compromise dimensional stability [63]. At the molecular level, Ms governs silicate speciation: lower Ms (higher alkalinity) favors highly reactive monomeric silicates that can generate a more porous gel network, whereas higher Ms introduces pre-polymerized silicate oligomers that function as nucleation "seeds" for polycondensation, promoting the development of a more cross-linked aluminosilicate framework associated with reduced permeability and higher ultimate strength [47, 64]. Consequently, this relationship follows an optimal threshold, typically lying within Ms 1–1.5, contingent upon the precursor type, to balance rapid dissolution kinetics with the structural integrity of the resulting gel matrix [24, 37, 47], making the Na_2SiO_3/NaOH ratio a primary control parameter governing the hardening profile of AAM systems [57].

Alkali concentration further dictates AAM performance and is commonly expressed as NaOH molarity or total Na_2O equivalent relative to the binder mass in percent. Higher molarity levels (10–14 M) increase pore solution alkalinity, thereby accelerating dissolution of the precursor's glassy framework through enhanced rupture of Si-O-Si and Si-O-Al bonds, which promotes rapid release of Si^{4+} and Al^{3+} species, shortens setting time, and enhances early-age strength [26, 62, 65, 66], an advantage for emergency pavement repair. However, this accelerated gelation can significantly reduce flowability and may compromise constructability [60, 67]. Lower molarity ranges (6–10 M) improve workability but slow reaction kinetics and strength development [26, 62, 67]. Similarly, Na_2O dosage, typically within the range of 2 to 12%, dictates the pH of the pore solution by providing the necessary H^- ions, which serves as the primary driver for dissolution kinetics [40, 47]. Increasing alkali content accelerates precursor dissolution and early gel formation; however, excessive dosages above approximately 8% may induce "alkali-overloading", characterized by rapid super-saturation and premature gel precipitation that encapsulates unreacted particles and restricts later stage reaction progress [40, 47]. Although higher Na_2O levels from 8 to 12% significantly refine the microstructure by reducing average pore size and total porosity, this densification is accompanied by elevated autogenous and drying shrinkage, thereby increasing the risk of interfacial delamination in overlay repair systems [12, 25, 39]. Conversely, lower dosages below 6% improve dimensional stability and economic efficiency by reducing shrinkage, but often fail to meet rapid pavement repair requirements due to insufficient dissolution, prolonged setting times, limited early age strength development, and compromised interfacial bonding [25].

While optimization strategies have been predominantly developed for conventional two-part AAM systems, their translation to field-scale pavement repair introduces practical constraints related to safety and constructability. In two-part systems, concentrated alkaline solutions must be pre-mixed and handled carefully to control exothermic heat release, and the transportation of corrosive liquids presents logistical and occupational hazards [60, 68]. These challenges have driven the development of one-part ("just add water") systems, in which solid activators are dry-blended with the precursor and activated solely through water addition. Common Na-based activators include powdered sodium silicate (e.g., sodium metasilicate pentahydrate) and sodium hydroxide flakes, whereas potassium carbonate and potassium hydroxide are typically employed in K-based formulations [22, 55, 56, 69, 70]. As illustrated in Figure 3, the fundamental distinction between two-part and one-part AAM systems lies in the mixing and delivery of the activator, with the latter offering improved handling and safety during field application.

In contrast to two-part systems, one-part AAMs rely on the *in-situ* dissolution of solid activators before polycondensation can proceed, resulting in a buffered and progressively increasing alkalinity. Dong et al. [70] showed that this mechanism delays and attenuates the main exothermic peak, extending the dormant period without compromising ultimate strength. However, the kinetics remain highly sensitive to activator characteristics, particularly particle size distribution, which governs the dissolution rate and subsequent pH rise. While finer particles accelerate early-age strength gain, they may intensify plastic shrinkage due to rapid chemical transitions [56, 69]. Thus, shifting from two-part to one-part systems does not eliminate the need for precise control of Ms and alkali dosage; rather, it redefines these parameters within a dissolution-controlled activation framework suited for safer field handling.

The chemical composition of the activator in one-part AAM dictates a critical trade-off between rapid-hardening and fresh-state workability. For example, potassium hydroxide with molarity levels of 12–16 M significantly accelerates polycondensation reactions in one-part UHGPC concrete, resulting in rapid-hardening but reduced flowability due to increased paste viscosity and a lower H_2O/alkali ratio [22]. This inverse relationship was also revealed by Dong et al. [70], who found that while higher dosages of solid sodium silicate increase early-age strength, they simultaneously increase paste viscosity, complicating handling. In contrast, activators

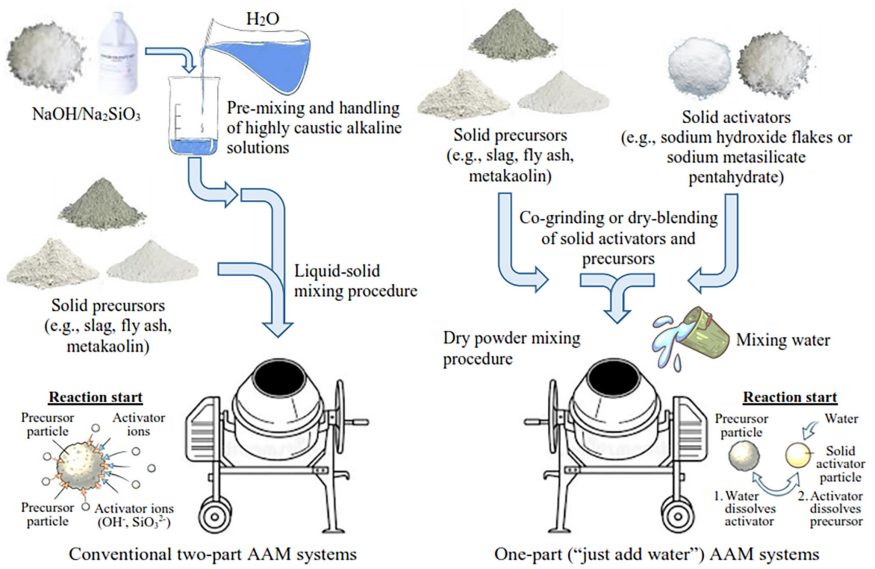

Figure 3 Schematic comparison of mixing procedures and activator delivery in two-part and one-part AAM systems

with slower dissolution kinetics, such as sodium carbonate, generally produce longer setting times and slower early-age strength gain [56]. To address the rheological limitations associated with highly alkaline systems, modifiers such as surfactants and salts of strong acids have been introduced to delay initial setting while maintaining high-early strength, particularly when combined with nanosilica [55]. Moreover, activator effects are strongly coupled with precursor chemistry: CaO-rich precursors promote rapid C-(A)-S-H gel formation and accelerate early-age strength, while supplementary silica-rich additives increase the Si/Al ratio and refine the gel network, and Class F fly ash tends to reduce early-age strength due to its slower dissolution [22, 55, 56].

3.2 Fresh and hardened properties in rapid pavement repair

3.2.1 Setting and flow characteristics

The success of rapid pavement repair hinges on balancing a sufficient "working window" for placement with a fast "setting time" to minimize lane closure duration, a balance fundamentally governed by the synergistic gel evolution discussed in Sections 3.1.1 and 3.1.2. According to ASTM C928, "Type R3" very rapid-hardening repair materials are often categorized by their ability to reach significant mechanical milestones within three hours, making the initial chemical induction period critical for meeting performance indicators. The reviewed AAM systems demonstrated considerable variability in these characteristics, largely controlled by the precursor's calcium availability and the activator's alkalinity.

Reported setting times span a wide range, with initial setting occurring as rapidly as 5 min [24, 25] and final setting extending beyond 200 min in some formulations [63]. While ultra-fast setting reduces traffic disruption, Yeo et al. [1] categorize such materials as "ultra-rapid" or "rapid" strength gain, noting that they pose a risk of "flash setting" during mixing; conversely, extended setting times delay the return to service beyond the thresholds specified for high-early strength concrete [5].

The setting behavior of AAM systems is fundamentally governed by Ca^{2+}-driven reaction kinetics, which control the rate of gel precipitation and structural stiffening. High-calcium precursors such as slag and Class C fly ash exhibit intense early reactivity due to their elevated CaO content, promoting rapid C-(A)-S-H gel formation and hardening within approximately one hour [25, 40, 45, 50]. For instance, ultra-fine slag activated with a $NaOH/Na_2SiO_3$ combination exhibits rapid-setting, with initial and final times of 11–13 and 22–24 min, respectively [41]. Alternatively, slag blended with portlandite and dihydrate gypsum, as well as slag-based AAMs activated with NaOH alone or combined with Na_2SiO_3 (4–12% Na_2O), exhibit broader setting time ranges, with initial and final setting occurring within 5–56 and 10–70 min, respectively [25, 40]. Within this range, an 8% Na_2O dosage serves as a threshold; increasing the dosage up to this point accelerates initial setting from 56 to 23 min, whereas further increases to 12% result in prolonged initial setting from 23 to 36 min [40], consistent with the mechanisms described in Section 3.2.2. Such rapid stiffening aligns with emergency repair requirements that require reopening to traffic within 4 to 8 h [5, 10]. However, excessive reaction rates significantly shorten the working window and may fail to satisfy the minimum 15-min consistency requirement for field placement [3], often necessitating the use of retarders or precursor blending to comply with BS EN 1504-3 provisions on adhesion and pot life for structural repair.

In contrast, low-calcium precursors such as Class F fly ash and metakaolin rely primarily on

slower N–A–S–H polycondensation mechanisms [21, 35, 37], frequently requiring heat curing to achieve practical setting times, which limits their suitability for *in-situ* pavement repair. To reconcile workability with rapid-hardening, hybrid systems regulate CaO availability through staggered ion dissolution pathways. Incorporation of Class F fly ash into a slag matrix has been shown to prolong setting times; specifically, each 10% increment in slag replacement potentially extends the setting process by approximately 5–10 min across various activator configurations [25, 41, 67, 71, 72]. Despite this delay, the setting times remain well within the three-hour limit specified by ASTM C928. Similarly, a comparable moderation of the hardening profile is observed in metakaolin-slag systems. Replacing slag with up to 15% metakaolin slightly prolongs setting [24], which facilitates enhanced reactivity at ambient temperatures while effectively mitigating flash setting [27]. This trend is further supported by studies on metakaolin blended with para wood or oil palm ash, which achieve high-early strength while maintaining adequate working time [54]. Collectively, these findings suggest that regulating CaO availability through precursor blending serves as a critical design variable for tailoring the setting time in rapid pavement repair applications.

Following the demonstrated influence of CaO availability on setting kinetics, workability emerges as an equally critical parameter in rapid pavement repair applications. The repair material must exhibit sufficient flowability to self-level and fill irregular pothole geometries without segregation, thereby meeting the bond strength and impermeability requirements for "Class R4" structural repairs under BS EN 1504-3. Activator composition plays a decisive role in governing the flow to setting transition. Specifically, mixtures with an elevated Ms or higher alkalinity tend to exhibit increased viscosity and diminished fluidity. Beyond the optimal thresholds discussed in Section 3.1.2, these parameters trigger accelerated silicate polymerization and rapid network formation pathway [40, 67, 73], which significantly impair workability. Such rheological stiffening poses a critical challenge for deep placement applications, as it hinders the uniform flow and compaction necessary for structural integrity. Particle geometry further modulates rheological behavior. The spherical morphology of fly ash particles promotes a ball bearing lubrication effect that enhances flow, whereas the irregular plate like structure of metakaolin increases water demand, internal friction, and reduces the effective working window [50]. To maintain the high fluidity required for self-compacting AAM mortars while preserving early-age strength development, chemical admixtures such polyvinyl alcohol latex powder and polypropylene fiber have been employed to prolonged the initial setting time of rapid-hardening binders, without compromising the 24-h strength targets specified in ASTM C928 [39, 74].

To consolidate the influence of key mixture variables on fresh-state behavior, Table 2 summarizes the combined effects of slag ratio, Ms, and Na_2O content on setting time and flowability across varying temperatures. In this dataset, slag content is defined as the mass fraction of total precursors (slag, Class F fly ash, and silica fume), Ms represents the SiO_2/Na_2O molar ratio of the activator, and Na_2O content is calculated relative to the activator solution, which differs from the Na_2O equivalent defined in Section 3.1.2; other parameters, including supplementary materials and liquid-to-solid ratio, are held constant. The results demonstrate a strong coupling between activator chemistry and temperature, where increasing temperature accelerates reaction kinetics, reducing setting time and flowability. Temperature acts as a key driver of the transition from workability to structural build-up through enhanced dissolution and condensation. Higher slag content intensifies this effect via rapid C-(A)-S-H formation, while Ms and Na_2O content control the balance between fluidity and early structuration. Mixtures with low Ms and high alkali concentration show delayed setting at low temperatures but become highly sensitive to thermal activation, indicating a shift in rate-controlling mechanisms. Three thermal regimes can be distinguished: at 20°C, reactions are dissolution-controlled, leading to extended workability but slow strength development; at 40°C, a catalytic threshold is reached, promoting concurrent C-(A)-S-H and N-A-S-H formation and providing an optimal balance between workability and early hardening; and at 60°C, reactions become diffusion-limited, resulting in rapid, flash-like setting that enhances early strength but increases the risk of autogenous shrinkage and interfacial microcracking due to accelerated heat release and moisture depletion [75]. This thermally driven structural evolution is further associated with increased yield stress and accelerated build-up in silicate-rich, high-alkali, slag-dominant systems [76].

3.2.2 Early-age strength

For rapid pavement repair materials, the key performance indicator is the ability to achieve a minimum opening strength, typically 20 MPa within a few hours to allow for same-day reopening to traffic. In terms of classification, ASTM C928 categorizes materials achieving ≥21 MPa in 3 h as "Type R3" very rapid-hardening repair materials, while BS EN 1504-3 sets a "Class R4" requirement for structural repairs at ≥45 MPa (28 days) with high early-age strength gain. Based on the review conducted, the AAM systems demonstrated superior early-age strength compared with Portland-based repair materials, primarily due to the rapid dissolution and polycondensation kinetics discussed in Sections 3.1.1 and 3.1.2, which mirror the characteristic of high-performance

Table 2 **Combined effects of slag ratio, Ms, Na_2O content, and temperature on the fresh-state behavior of AAM systems, adapted from Qian et al. [75]**

Temperature (°C)	Slag ratio	Ms	Na_2O (%)	Setting time (min)		Flowability (cm)
				Initial set	Final set	
20	0.25	1.8	9	29	35	19.5
	0.50			26	30	19.4
	0.75			23	27	19.1
	1.00			19	24	17.7
	0.5	0.6		212	232	18.1
		1.2		22	27	20.9
		2.3		696	1171	14.5
		1.8	5	72	76	18.4
			7	35	40	18.8
			11	20	27	21.6
			13	25	35	20.5
40	0.25		9	22	28	19.1
	0.50			18	24	18.7
	0.75			17	23	18.3
	1.00			15	20	17.1
	0.5	0.6		187	231	16.8
		1.2		15	23	19.9
		2.3		494	649	13.4
		1.8	5	58	65	17.7
			7	23	31	18.1
			11	16	22	20.4
			13	18	24	20.2
60	0.25		9	20	27	18.7
	0.50			15	21	18.5
	0.75			13	19	18.1
	1.00			13	16	16.1
	0.5	0.6		165	214	14.5
		1.2		13	19	19.7
		2.3		287	592	12.5
		1.8	5	43	53	17.6
			7	21	25	17.9
			11	14	20	20.1
			13	16	21	20.0

cementitious systems used in "Sprint" fast-setting technologies [10].

As established in Section 3.1.1, slag-based and hybrid slag-containing systems consistently demonstrate exceptional early-age strength under ambient curing conditions, fulfilling the practical requirement for "cold" field applications where external heating is impractical. Slag-based AAM, for instance, achieved approximately 30 MPa within one day [26, 40, 41], without additional heat treatment, in contrast to Class C fly ash, which requires heating at 70°C to achieve equivalent compressive strength in the same time, even though both are categorized as CaO-rich precursors. For rapid pavement repair, this advantage becomes more pronounced: optimized slag-containing mixtures have been reported to reach 16–28 MPa within 6–8 h [22, 27, 70, 77] and exceed 45 MPa at 24 h through appropriate adjustment of precursor and activator formulations [36, 70–72, 78]. These strength levels are sufficient to enable overnight or same-day traffic reopening and satisfy the minimum 45 MPa requirement for "Class R4" structural repair materials specified in BS EN 1504-3.

As illustrated in Figure 4, a positive correlation was observed between the slag content in the hybrid AAM systems and the 24-h compressive strength. Within the studied range, a higher slag proportion generally improved the early mechanical performance, likely due to increased CaO availability and accelerated C-(A)-S-H gel formation. Mixtures containing more than 60% slag achieved compressive strengths exceeding 40 MPa at 24-h, thus exceeding the ≥20 MPa threshold generally adopted for early traffic reopening. Although early-age strength is not uniformly reported, the typical nonlinear strength gain of slag-rich AAMs suggests that the 20 MPa criterion can be achieved in approximately 6–12 h under favorable conditions. However, these projections remain sensitive to temperature and mix design, necessitating verification through

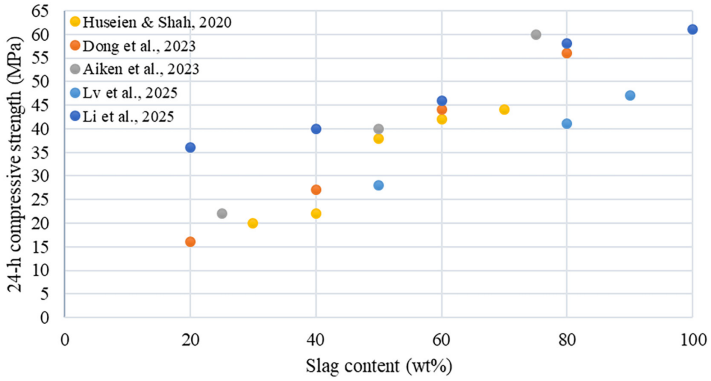

Figure 4 Influence of slag content on the 24-h compressive strength of hybrid AAM systems [36, 50, 70–72]

early-age strength monitoring or maturity-based controls to avoid overestimating *in-situ* performance.

The efficacy of these systems is further enhanced through ultra-high-early strength AAM formulations. Hybridization strategies such as the partial substitution of metakaolin with biomass ashes, including para wood or oil palm ash, accelerate initial hardening and facilitate early reopening to traffic [54]. This acceleration is primarily attributed to the additional reactive silica and alkali content within the biomass ash, which intensifies the dissolution-condensation process. While thermal curing is known to catalyze strength gain, its large-scale application in pavement repair remains logistically challenging. As noted by Yeo et al. [1], repair materials are classified by their strength-gain rates from ultra-rapid to normal; for AAMs to achieve "ultra-rapid" status under ambient conditions, the chemical synergy between the precursor and activator is paramount. Nonetheless, emerging techniques like electrothermal curing offer a compromise for localized repairs; Balapanov et al. [51] demonstrated that applying 40 V yielded 31.34 MPa in only 4 h. In the absence of such interventions, ambient curing of Class F fly ash-based AAMs, which lack sufficient reactive Ca^{2+} as detailed in Section 3.1.1, typically leads to sluggish reaction kinetics and delayed strength development [35], underscoring the need to incorporate a substantial slag fraction to stimulate hardening at an early age.

As detailed in Section 3.1.2, activator chemistry must be precisely calibrated. Ji et al. [40] reported that while optimal alkalinity (Na_2O eq. ≈ 8.0%) produced high strength, excessive alkalinity hindered polymerization and caused embrittlement and cracking, a failure mode that would be catastrophic under repetitive traffic loads. This aligns with findings that excessively high NaOH Molarities (e.g., 16 M) can promote premature calcium precipitation, leading to a porous, weaker matrix [65]. These findings underscore that early strength is not governed solely by reaction rate, but by achieving a controlled balance between dissolution and stable polycondensation through appropriate Ms and alkali dosage.

Temperature further governs reaction kinetics and directly influences the feasibility of early traffic reopening. Rather than merely shifting reaction stages, temperature alters the reaction degree. At 20°C, which represents typical nighttime or early-morning field conditions, Class F fly ash remains largely unreacted (inert filler), limiting early strength. In contrast, at 40 to 60°C, commonly encountered during daytime construction in warm climates or at midday under intense solar radiation and elevated pavement temperatures, Class F fly ash becomes activated and contributes synergistically with slag to form a denser matrix, significantly enhancing early-age performance. From a calorimetric perspective, this transition is reflected in the acceleration stage of heat evolution, which governs the formation rate of the primary load-bearing gel network [75, 76]. Systems with earlier and steeper heat release peaks generally achieve faster strength gain, which is essential for rapid pavement repair. However, excessive acceleration can lead to heterogeneous gel formation and shrinkage-induced microcracking, thereby compromising the repair's long-term durability.

3.2.3 Bonding to existing concrete substrate

The structural integrity and service life of a pavement patch are fundamentally dependent on the quality of the bond between the repair material and the existing concrete substrate. In rapid pavement repair, bond failure typically manifests as delamination or "pop-out" caused by high shear and impact stresses from rolling wheel loads. For a repair to be deemed effective, it must satisfy specific performance indicators; for instance, BS EN 1504-3 mandates a bond strength of ≥2 MPa for "Class R4" structural repairs, while ASTM C928 sets a more rigorous one-day benchmark of ≥7 MPa for "Type R3" very rapid-hardening repair materials.

The reviewed AAMs consistently meet or exceed relevant regulatory requirements, highlighting the importance of optimizing both precursor blend and activator chemistry to maximize interfacial adhesion. In hybrid slag-Class F fly ash systems, interfacial bond strength shows

a non-linear dependence on slag content, with optimum performance typically around 50% slag. Fan et al. [20] reported bond improvements exceeding 62% relative to OPC at this composition, while Zhang et al. [79] observed peak splitting tensile strength of about 2.4 MPa at 50% slag compared with 1.4–1.8 MPa at lower or higher replacement levels. This trend indicates that intermediate slag contents provide balanced gel chemistry and shrinkage compatibility, improving chemical adhesion and mechanical interlocking at the repair interface. Using modified slant shear and pull-off tests, early-age bond strengths of approximately 7–10 MPa at three days have been reported for slag-Class F fly ash AAM systems [26], whereas slag-metakaolin-Class F fly ash blends show lower interfacial flexural tensile strength of around 2.1 MPa at the same age [50], illustrating the influence of precursor chemistry and test configuration. Nevertheless, optimized metakaolin-based AAM mixtures containing 30% slag can still achieve adequate early-age bonding strength, reaching about 3.7 MPa at 1 day and 6.42 MPa at 28 days [27]. Complementing precursor optimization, studies indicate that a composite activator combining Na_2SiO_3 and NaOH resulted in a denser interfacial microstructure, underscoring the critical role of activator chemistry in ensuring the durability of AAM-based repairs [61, 68].

The superior interfacial performance of AAM repairs originates from a chemically integrated ITZ rather than a mechanically dependent contact zone. As discussed in Sections 3.1.1 and 3.1.2, the precursor-activator synergy enables a reactive interface in which the highly alkaline pore solution penetrates the OPC substrate, dissolving portlandite and residual C-S-H phases [20, 59, 61]. This dissolution induces bi-directional ionic migration, with Ca^{2+} diffusing into the AAM matrix and Si^{4+}, Al^{3+}, and alkali cations migrating toward the existing OPC substrate [20, 50, 56, 59, 68]. The resulting ionic exchange promotes *in situ* precipitation of C-(A)-S-H and cross-linked aluminosilicate frameworks across the interface, effectively creates a continuous "chemical bridge" that chemically binds the two distinct matrices together [79, 80]. In contrast to conventional OPC repairs, where the "wall effect" often produces a porous and mechanically weak ITZ, AAM systems generate a densified interphase with refined pore structure [50, 81, 82]. Microhardness gradients demonstrate a gradual strength transition rather than a distinct weak plane, in some cases exceeding the adjacent OPC matrix [79–81]. Importantly, this interfacial densification reduces permeability and limits the ingress of water and de-icing salts, thereby mitigating freeze-thaw deterioration and enhancing long-term pavement durability [20, 59, 68].

While AAMs are capable of forming a chemically integrated ITZ, the extent of this interfacial densification remains highly dependent on substrate preparation and field execution. To effectively translate the intrinsic chemical advantages of AAM binders into durable pavement repairs, careful management of substrate conditions is essential. Mechanical surface treatments such as sandblasting or grooving enhance surface roughness and increase effective contact area, supporting both chemical bonding and mechanical interlocking. Moisture control is particularly critical for AAM repairs: unlike OPC where a saturated surface dry condition is standard, excessive moisture may dilute the alkaline activator and reduce local pH at the interface, whereas an overly dry substrate can absorb the activator and hinder polymerization reactions. Current evidence suggests that a slightly dry condition provides a more favorable balance, allowing adequate activator penetration without significant dilution [50, 83, 84]. Repair geometry further influences stress transfer efficiency, as interlocking rectangular or mortise-tenon cuts improve tensile performance relative to conventional rectilinear forms [59]. The incorporation of modifiers such as polyvinyl alcohol latex, polypropylene fibers, or epoxy resin can additionally enhance crack-bridging capacity and interfacial toughness under cyclic traffic loading [74, 85, 86].

3.3 Durability-related properties

3.3.1 Shrinkage and creep behaviors

The long-term suitability of AAMs for rapid pavement repair is strongly governed by volumetric stability, as excessive deformation directly compromises interface bond durability between the repair layer and the existing concrete substrate. Performance specifications such as ASTM C928 therefore impose strict limits on length change, typically below 0.15% at 28 days, to prevent debonding and premature failure. Existing literature consistently highlights a fundamental distinction in shrinkage and creep mechanisms between high- and low-calcium systems [12, 87], arising from differences in gel chemistry and pore structure evolution, as discussed in Sections 3.1.1 and 3.1.2.

In high-calcium systems, particularly slag-based, volumetric instability is predominantly governed by autogenous mechanisms rather than external drying. Rapid hydration consumes pore solution, generating self-desiccation and capillary stresses within an increasingly refined pore network. The dense microstructure and high surface tension of the alkaline pore solution amplify internal capillary pressures, while the viscoelastic nature of C-(A)-S-H gels renders the solid skeleton susceptible to deformation under tensile stress [12, 42, 44]. Additional contraction arises from chemical polycondensation and reduced steric-hydration repulsion as ionic concentrations evolve. Collectively, these mechanisms promote micro-cracking even before service loading, posing a risk to dimensional stability requirements such as those defined in BS EN 1504-3. Reported

drying shrinkage values of 600–1200 microstrain at 90 days typically exceed those of OPC systems, underscoring the intrinsic shrinkage sensitivity of slag-based matrices [12].

In contrast, shrinkage in low-calcium systems dominated by Class F fly ash is primarily governed by moisture transport rather than intense self-desiccation. Slower reaction kinetics and a coarser pore structure result in lower early stiffness, reducing resistance to tensile stresses induced by drying. The N-A-S-H gel network retains a greater proportion of physically bound water, making evaporation-driven contraction the principal shrinkage mechanism [12, 36]. While this open pore network may lead to elevated early-age drying shrinkage, stabilization generally occurs more rapidly than in slag-rich matrices due to the formation of a comparatively rigid cross-linked C-(A)-S-H network.

Time-dependent deformation further compounds durability concerns in high-calcium systems. Slag-rich binders typically exhibit higher Ca/Si ratios within the C-(A)-S-H gel, producing a less polymerized silicate network than the N-A-S-H framework in low-calcium systems. This structure reduces gel packing density and increases interlayer and physically bound water, facilitating viscous sliding and nanoscale rearrangement under sustained load. Consistent with this mechanism, Hojati et al. [87] reported creep coefficients of 3.6–4 after 20 months at 40% of compressive strength for slag-based binders, substantially higher than 1.9–2.6 for Class F fly ash-rich systems and 1.1 predicted for OPC by ACI 209 models. Similar trends were observed by Caron et al. [88] for slag-based AAM concrete, where basic creep after 100 days was approximately twice that of OPC and continued increasing at later ages, which indicates that conventional prediction models, including fib Model Code formulations, significantly underestimate creep in slag-rich systems unless basic creep compliance is increased by roughly 2 to 3 times [88]. This divergence from OPC-based predictions highlights the prolonged viscoelastic relaxation in C-(A)-S-H gels with higher Ca/Si ratios, whereas low-calcium systems, characterized by more cross-linked N-A-S-H networks and lower Ca/Si ratios, tend to approach deformation equilibrium earlier [87, 88]. From a pavement repair perspective, such rheological incompatibility between an AAM repair layer and an OPC substrate may lead to differential strain accumulation, stress redistribution, joint opening, slab curling, and progressive surface distress under cyclic traffic loading.

These contrasting mechanisms indicate that shrinkage in high-calcium systems is predominantly chemically driven and governed by self-desiccation, whereas in low-calcium systems it is largely moisture-transport controlled, underscoring the need for composition-specific mitigation strategies in durability-critical applications. To control shrinkage and creep-related instabilities in high-calcium systems, micromechanically informed hybridization is required. Incorporating low-CaO precursors into slag-based matrices reduces the effective Ca/Si ratio and moderates rapid C-(A)-S-H precipitation, thereby alleviating abrupt pore refinement and excessive capillary stress development. Aiken et al. [36] showed that Class F fly ash delays slag reactivity, promoting more gradual gel formation and controlled microstructural densification. This moderated reaction pathway limits self-desiccation-induced tensile stress while maintaining sufficient gel connectivity to preserve mechanical performance, ultimately reducing both autogenous shrinkage and long-term viscoelastic deformation.

While precursor hybridization stabilizes high-calcium systems, internal stability remains sensitive to activator chemistry. Generally, increasing Ms enhances shrinkage in both systems via pore refinement, whereas higher alkalinity accelerates shrinkage in high-calcium systems but reduces it in low-calcium systems by increasing structural stiffness. Further dimensional stabilization can be achieved through targeted chemical and moisture-control strategies that rebalance internal stress development. CaO-rich shrinkage-reducing agents hydrate at early ages to induce controlled chemical expansion, counteracting autogenous shrinkage strains [89]. When properly dosed, these Ca-bearing phases may also refine pore structure; however, excessive expansion can introduce microcracking, highlighting the need for dosage optimization. In parallel, Class F fly ash blended with sulfate-containing additives and $Ca(OH)_2$ promotes the formation of mildly expansive aluminosilicate hydrates under saturated conditions, partially compensating for slag-induced shrinkage through microstructural stress redistribution rather than external restraint [4, 90]. Complementing chemical expansion, internal curing via Superabsorbent Polymers (SAPs) provides moisture-regulated shrinkage control. By acting as distributed water reservoirs, SAPs sustain internal relative humidity and moderate capillary pressure development during self-desiccation [43]. This controlled moisture supply reduces early-age shrinkage and limits capillary-driven gel densification, which is closely related to the creep evolution in C-(A)-S-H gels with high Ca/Si ratios.

3.3.2 Resistance to environmental factors

The long-term performance of rapid pavement repairs depends not only on early-age strength but on resistance to aggressive exposure conditions, as reflected in durability requirements such as BS EN 1504-3 and ASTM C928. Compared with OPC systems, AAMs generally exhibit enhanced environmental resilience [13, 29, 62, 91, 92], primarily due to their refined pore structure and chemically stable aluminosilicate networks, which

restrict the transport of deleterious ions. Rather than uniformly superior performance, however, durability depends strongly on precursor chemistry and gel composition.

Chloride and Water Penetration: AAM systems generally exhibit lower chloride permeability and water absorption than OPC systems due to their refined pore structure, reduced capillary pore connectivity, and the formation of a dense, cross-linked aluminosilicate network [22, 91, 93, 94]. Slag-based and hybrid slag-containing systems consistently demonstrate reduced chloride migration coefficients and sorptivity values compared to OPC systems [20, 62, 92, 95, 96], primarily as a result of enhanced matrix densification and chemical chloride binding within aluminosilicate frameworks. However, for specific rapid pavement repair applications, chloride resistance must be interpreted beyond intrinsic permeability metrics [20, 59]. Repair overlays are typically thin and bonded to chloride-contaminated substrates, creating a risk of interfacial chloride accumulation and differential transport. Moreover, early-age exposure to moisture and de-icing salts before complete gel maturation may increase transient permeability, particularly in systems with high alkali dosage. While the long-term transport resistance of slag-rich AAMs is promising [96], their performance under early traffic reopening, restrained geometry, and cyclic wetting-drying typical of pavement environments remains insufficiently quantified, indicating that transport properties should be evaluated under field-simulated boundary conditions rather than standard bulk diffusion tests alone.

Sulfate and Acid Resistance: AAMs demonstrate superior resistance to sulfate and acid attack compared to OPC, largely due to their distinct gel chemistry and absence of portlandite-rich phases [15]. After immersion in Na_2SO_4, both one-part and two-part AAM systems exhibit significantly lower strength loss compared to OPC controls [15, 92]. Unlike OPC, where sulfate exposure induces expansive ettringite and gypsum formation, Na_2SO_4 interaction in AAM matrices is generally non-expansive and may sustain pore solution alkalinity, particularly in low-calcium systems that lack reactive Ca phases [13, 19]. Nevertheless, remains aggressive due to Mg^{2+}-induced decalcification of C-(A)-S-H gels, forming brucite and non-cementitious M-S-H phases that compromise structural integrity [13, 15, 19]. Regarding acid resistance, low-calcium AAM systems experience substantially less strength loss in sulfuric acid compared to the severe degradation observed in OPC [15, 65, 92], with research indicating minimal damage to the AAM matrix relative to the extensive paste dissolution found in OPC samples [28]. While these findings confirm the chemically driven durability advantages, rapid pavement repair applications introduce additional complexities, including thin bonded sections, shrinkage constraints, and exposure to sulfate-bearing groundwater, which, combined with traffic-induced cracking at the repair-substrate interface, can accelerate ion ingress despite stable matrix chemistry.

Freeze-Thaw Resistance: Freeze-thaw resistance in AAMs exhibits considerable variability, governed by pore structure, gel chemistry, and air void characteristics. Slag-rich AAMs generally demonstrate high durability with minimal mass loss [13, 29], whereas metakaolin-based AAMs can show significant weight and relative dynamic modulus loss when lacking air entrainment [37]. Higher alkali concentrations and increased slag content promote dense C-(A)-S-H-rich matrices with reduced freezable water and lower permeable porosity, thereby mitigating hydraulic expansion during freezing [22, 60, 68]. Moderate slag incorporation appears to optimize durability in hybrid slag-Class F fly ash systems [68], as higher slag content is associated with improved residual compressive strength [71]. Damage typically follows a two-stage pattern characterized by rapid early Ultrasonic Pulse Velocity (UPV) loss and subsequent gradual degradation [68]. However, for specific rapid pavement repair, the critical concern is early-age freeze exposure before complete reaction and pore refinement. Thin repair layers may reach critical saturation more rapidly than bulk specimens, and differential thermal movement between repair and substrate can induce interfacial debonding under cyclic freezing. Additionally, freeze-thaw performance under de-icing salt scaling and simultaneous traffic loading remains underexplored for AAM-based repair materials.

Abrasion Resistance: AAMs generally demonstrate strong abrasion resistance relative to OPC systems, largely attributed to their dense gel structure, refined pore network, and strong matrix-aggregate interfacial bonding, which enhance surface hardness and reduce aggregate pull-out during mechanical wear. The early formation of cross-linked aluminosilicate networks contributes to improved cohesion within the ITZ, supporting greater resistance to surface degradation in comparison with OPC concrete [28, 62]. Abrasion resistance in AAM systems is also closely linked to mechanical performance and microstructural characteristics, particularly compressive and split tensile strength as well as overall porosity [60]. Improvements in wear resistance have been associated with optimized precursor compositions, especially through increased slag content in hybrid systems that promote matrix densification and stronger interfacial bonding [27, 71]. Additionally, the inclusion of fibers in Class F fly ash-based AAM repair materials can enhance crack control and improve resistance to abrasion-related deterioration, further supporting their suitability for pavement repair applications subjected to repeated mechanical loading [85]. Nevertheless, rapid pavement repairs experience intense early traffic loading and stress concentrations at patch boundaries, meaning standard long-term test values may not accurately represent performance

during the critical first 24–72 h when early traffic reopening is required.

3.4 Applicability of the maturity method for AAMs field control

To translate the rapid and complex reaction kinetics of AAM systems identified in Section 3.1 into actionable field decisions, the maturity method has been validated as a reliable non-destructive technique. This method correlates the cumulative curing temperature-time history (maturity index) with the mechanical strength gain, providing a practical mechanism to verify whether the critical opening strengths defined in Section 3.2.2 have been achieved under variable field conditions [97–100]. Its robust applicability extends across the spectrum of precursors previously identified, including Class F fly ash, slag, and hybrid (binary) blends, offering essential strength-maturity relationships for both mortars and concrete [97–99].

The different reaction kinetics of the precursors identified in Section 3.1.1 directly dictate the selection of an appropriate maturity function. However, traditional models often fall short for certain AAM systems. For low-calcium systems dominated by polymerization (e.g., Class F fly ash), conventional Arrhenius models can fail to capture the disproportionately large impact of early-stage maximum curing temperatures. To address this, Shin et al. [99] demonstrated that a novel "Weighted Maturity" function is required to accurately model these thermally activated, nonlinear dissolution processes ($R^2 > 0.94$), directly challenging the commutative assumptions of standard maturity indices. In contrast, high-calcium systems rich in slag, which Section 3.2.1 noted as having rapid-setting times, exhibit a more predictable strength-temperature interaction. In slag-OPC mixtures, the optimal effective datum temperature (T_0) for the Nurse-Saul function was found to be −3°C [100], a notably higher threshold than the common value of −10°C, reflecting the suppression of the latent hydraulic reactions of slag near the freezing point.

Accurate maturity-based predictions for rapid pavement repair depend on the precise determination of T_0, which represents the theoretical threshold below which strength development ceases, and the apparent activation energy (Ea), which quantifies the energy required to initiate and accelerate chemical reactions. Unlike OPC, AAM systems exhibit wider variability in these parameters due to diverse precursor chemistries and reaction pathways. Class F fly ash-based AAMs typically require very high T_0 (e.g., >40.6°C) and exhibit Ea ranging from about 51.1–92.4 kJ/mol, indicating strong temperature dependence and limited reactivity at ambient conditions without external heating [97,98]. In contrast, slag-rich AAMs shift the T_0 down to manageable ambient ranges (around 2.7°C), enabling effective reaction at typical field temperatures [98]. Their Ea, commonly near 40 kJ/mol, is comparable to that of OPC [99], suggesting similar energy requirements for initiating reactions while still enabling high-early strength through rapid C-(A)-S-H formation. These differences highlight that maturity parameters for AAM systems cannot be directly adopted from OPC and must be calibrated according to precursor chemistry.

Despite the chemical complexities of these varied precursors, the temperature-dependent early-age strength gain (in the 5–10 MPa range) remains reasonably predictable using S-shaped curve models (Plowman, Logistic, Gompertz), yielding prediction errors within approximately 10% [100]. However, the method has historically faced limitations relevant to the early "working window" discussed in Section 3.2.1. While prediction errors using traditional logarithmic models (like Plowman) increase substantially in the very early 3–5 MPa range due to initial chemical variability, the Gompertz mathematical model has proven superior, accurately predicting this critical 3–5 MPa threshold essential for early formwork removal and preliminary traffic opening [100]. For determining later, full "traffic reopening" thresholds (e.g., ≥20 MPa), reliability improves significantly across all models, with errors for mortar and concrete AAMs typically dropping below 10% as curing progresses and the matrix stabilizes.

Table 3 summarizes maturity formulations from the literature, highlighting their specific roles in predicting the early-age strength development required for rapid pavement repairs.

3.5 Field applications and case studies

Only a limited number of investigations have reported pilot- or full-scale field applications of AAMs in pavement and structural repair, yet these trials have consistently demonstrated the feasibility of such systems for patching and rehabilitation. The principal objective in these studies was to achieve a rate of strength development sufficient to permit reopening to traffic within the same day, a performance target originally outlined in pioneering field repair trials on optimized metakaolin-based AAM mortars [54].

Laboratory-scale studies confirm the feasibility of this approach, showing that optimized AAM formulations can achieve target compressive strength within hours under ambient curing. Field deployments further support these material-performance relationships, although their success depends on maintaining consistency between laboratory optimization and site-specific boundary conditions. As discussed in Sections 3.2.1 and 3.2.2, careful adjustment of precursor-activator formulations, particularly through blending slag with metakaolin or Class F fly ash, enables a balance between flowability and fast setting, facilitating high-early strength without external heat curing [27, 50, 73]. However, accelerating reaction kinetics may narrow the workable time window and increase early shrinkage susceptibility, necessitating careful mix design control. Beyond rapid-hardening,

Table 3 **Summary of maturity formulations and synthesized analytical insights from the literature for AAMs field control**

Reference	Maturity Formulations	Synthesized Insights
Ferreira et al. [97]	*Nurse-Saul:* $M(t)=\sum_0^t (T_a - T_0)\cdot \Delta t$ *Arrhenius:* $t_e=\sum_0^t e^{\frac{E_a}{R}\left(\frac{1}{T_a}-\frac{1}{T_s}\right)}\cdot \Delta t$	Class F fly ash-based AAMs exhibit very high datum temperatures ($T_0 \approx 42.7$°C), indicating strong thermal activation. Conventional maturity models therefore perform poorly under ambient curing, limiting their suitability for rapid pavement repair without external heating.
Shin et al. [99]	*Weighted Maturity:* $M_w \doteq \sum_{k=1}^{N} W(T_{max}, t_k)\cdot (T_k - T_0)\cdot \Delta t$ *(Where W is a specific weight function capturing the coupled effects of maximum early-age temperature and duration.)*	Incorporating temperature-weighting functions improves prediction accuracy by capturing the combined effects of peak temperature magnitude and duration. This approach better represents nonlinear early-age reaction kinetics than linear Nurse-Saul assumptions.
Kim & Lee [100]	*Nurse-Saul:* $M(t)=\sum_0^t (T_a - T_0)\cdot \Delta t$ *Plowman:* $S = a + b\log(M)$ *Logistic:* $S=\frac{F_\infty}{1+exp(-K\cdot\log(M)+m)}$ *Gompertz:* $S = F_\infty \cdot \left(exp\left(-a\left(1/M\right)^b\right)\right)$	Slag-blends exhibit synergistic reactivity, enabling early strength development at ambient temperatures. The Gompertz model shows strong predictive capability for the critical 3–5 MPa strength range required for opening to traffic. However, the optimal datum temperature ($T_0 \approx -3$°C) differs from the ASTM default of −10°C, highlighting the need for system-specific calibration.
Abdulmajid et al. [98]	*Nurse-Saul:* $M(t)=\sum_0^t (T_a - T_0)\cdot \Delta t$ *Arrhenius:* $t_e=\sum_0^t e^{\frac{E_a}{R}\left(\frac{1}{T_a}-\frac{1}{T_s}\right)}\cdot \Delta t$	Strong precursor dependency is observed: Class F fly ash-based AAMs require 40°C curing, whereas slag-based AAMs gain strength at 5–40°C. Large variability in T_0 values highlights the need for mix-specific maturity calibration.

the structural reliability of repair patches critically depends on interfacial bond performance (Section 3.2.3), especially under restrained conditions where differential shrinkage and thermal gradients may induce debonding stresses. Although the transition toward safer one-part ("just add water") systems has revealed adhesion limitations in some single-precursor formulations, hybrid precursor strategies have been shown to substantially enhance chemical and volumetric compatibility with aged OPC substrates [56, 69, 101]. Ultimately, sustained field performance is governed not only by early-age strength gain but also by dimensional stability (Section 3.3.1) and resistance to aggressive environmental (Section 3.3.2), underscoring that successful rapid pavement repair requires an integrated balance between reaction kinetics, bond integrity, and long-term durability.

Complementary full-scale implementations further substantiate the technical feasibility of AAMs under demanding service conditions while also revealing scale-dependent challenges. A prominent example is the construction of heavy-duty pavements at Brisbane West Wellcamp Airport, where approximately 40,000 m³ of slag-based AAM concrete incorporating Class F fly ash and silica fume was successfully produced and placed [28]. Beyond demonstrating logistical scalability, this project confirmed that AAM systems can satisfy stringent flexural strength specifications while reportedly achieving substantial reductions in embodied carbon relative to OPC concrete. Similarly, Chen et al. [27] documented a campus road repair in which metakaolin-slag AAM mortar enabled traffic reopening within 6 h without observable cracking or debonding after one-year, illustrating the compatibility between early-age strength gain and interfacial stability. Additional pilot- or full-scale studies consistently report rapid-setting times and satisfactory one-day compressive strengths, indicating that laboratory-optimized kinetics can be translated to practice when mixture control is maintained [72, 73].

Despite promising outcomes, field-based studies highlight several implementation challenges, including achieving uniform mixing and activator distribution during large-scale batching as well as balancing workability with fast setting behavior. Although high-modulus soluble silicates can extend workable time while maintaining early-age strength [8], temperature sensitivity, early-age shrinkage under restrained conditions, and reliable curing control under fluctuating ambient environments remain critical concerns, particularly for early-opening decisions. In this context, maturity-based prediction provides a useful decision-support framework for managing thermal variability in complex AAM systems. As discussed

in Section 3.4, mixture-specific advanced maturity models, such as the "Weighted Maturity" function, can improve confidence in real-time strength estimation and reduce the risk of premature loading.

4 Discussion

4.1 Synthesis of evidence on the potential of AAMs for rapid pavement repair

The viability of rapid pavement repair materials is governed by three key performance criteria essential for early traffic reopening and long-term structural reliability. First, speed of strength gain is critical to achieving adequate load-bearing capacity; specifically, reaching ≥20 MPa within a few hours to align with ASTM C928 "Type R3" standards (≥21 MPa at three hours), while maintaining a minimum workability window of approximately 15 min for field placement [1–3, 5, 10]. Second, interfacial bond integrity ensures effective stress transfer with the existing substrate. This typically necessitates a tensile bond strength of ≥2 MPa as specified in BS EN 1504-3 for "Class R4" and a one-day slant-shear strength of ≥7 MPa as specified in ASTM C928 "Type R3" (or Type R2/R1 depending on the specific standard). Third, long-term durability involves resistance to environmental stressors such as chloride ingress, freeze-thaw cycles, and de-icing chemicals to prevent premature failure [1]. To this end, BS EN 1504-3 mandates a chloride content limit of ≤0.05%, while ASTM C928 restricts 28-day drying shrinkage to ≤0.15% to mitigate cracking. Beyond these mechanical requirements, sustainable infrastructure initiatives highlight secondary factors such as constructability, carbon footprint reduction, and cost-effectiveness [1,2].

Speed of Strength Gain: Synthesized evidence indicates that CaO-rich mixtures, particularly slag-based and hybrid slag-containing binders, consistently meet this operational threshold. Under ambient curing conditions, slag-based AAMs commonly develop compressive strengths of around 30 MPa within one day [26, 40, 41]. For practical repair scenarios, optimized slag-containing mixtures typically achieve about 16–28 MPa within 6–8 h and exceed 45 MPa at 24 h through appropriate precursor-activator formulations [22, 27, 36, 70–72, 77, 78], enabling early reopening to traffic. This performance is comparable to or higher than that of alternative rapid-repair binders such as MPC, which generally develops approximately 16 MPa at 6 h [14]. In parallel, the initial and final setting times reported for slag-based AAM systems typically range from approximately 5–56 min and 10–70 min, respectively [25, 40], which can then be slightly prolonged by hybridization [25, 41, 67, 71, 72], in accordance with the practical working time windows generally specified for rapid-repair materials [3]. Emerging accelerated curing approaches, including electrothermal and pulsed microwave curing, further demonstrate the potential to ensure rapid strength development even under low-calcium or cold-weather conditions [21, 51].

Interfacial Bond Integrity: Synthesized evidence demonstrates that the enhanced interfacial ITZ characteristics described in Section 3.2.3 translate directly into reliable field performance, effectively mitigating the primary failure mode of pavement patch repairs, namely debonding. Field implementation reported by Chen et al. [27] showed no visible cracking or delamination after one year of service, supported by early tensile bond strengths of about 3.7 MPa at one day. Laboratory investigations further report bond strengths of approximately 7–10 MPa at three days for slag-Class F fly ash AAM systems using modified slant shear and pull-off tests [26], although measured values depend on precursor chemistry and test configuration. In comparison, OPC repair materials often struggle to maintain bond strengths above approximately 1.5 MPa without specialized bonding agents [82], whereas although MPC provides rapid-setting, its interface with existing concrete may deteriorate under wet-dry cycling due to dissolution of residual phosphate phases [14]. Additional improvements can be achieved through interface optimization strategies, including bonding agents that increase tensile bond strength and repair geometries such as mortise-tenon configurations that enhance stress transfer efficiency [59, 79].

Long-Term Durability: Synthesized evidence indicates that AAM-based repair materials can enhance long-term pavement durability due to the formation of dense cross-linked aluminosilicate networks that provide greater resistance to environmental stressors than OPC-based. Although slag-rich AAMs may initially exhibit elevated drying and autogenous shrinkage, this risk can be effectively mitigated through mixture design and curing strategies. Hybridization with Class F fly ash has been shown to reduce autogenous shrinkage by up to 75% [63], while the incorporation of SAPs and polymer fibers can mitigate plastic and drying shrinkage cracking [43, 83]. Optimized curing regimes, such as heat curing around 40°C or extended curing duration, may further reduce drying shrinkage by up to 40% [36]. In terms of chemical durability, AAMs demonstrate substantially lower transport properties than OPC, with slag-based mortars exhibiting chloride migration coefficients up to 10 times lower and water penetration depths only about 12.8% of OPC, largely due to their refined pore structure [42]. These systems also show enhanced resistance to aggressive environments, including sulfuric acid and sulfate exposure, with significantly lower strength loss compared to OPC [92]. In addition, optimized slag-containing mixtures exhibit strong resistance to physical deterioration mechanisms, surviving approximately 300–1300 freeze-thaw cycles with minimal mass loss (<1%) and demonstrating improved abrasion resistance, with wear depths reported up to 61% lower than OPC [27–29, 60, 62].

The transition to sustainable infrastructure initiatives strongly favors AAMs by addressing critical environmental and economic factors alongside superior mechanical and durability performance. Primarily, AAMs utilize industrial by-products such as slag and fly ash as precursors, serving as a low-carbon alternative to OPC capable of achieving up to a fourfold reduction in CO_2 emissions [11]. This approach supports circular economy principles by valorizing abundant local waste streams [28], thereby reducing raw material expenditures. Economically, AAMs offer substantial advantages; recent analyses indicate that hybrid systems can be 5 to 9 times more cost-effective than conventional commercial polymer-modified repair mortars while meeting standard strength requirements [15].

4.2 Integrating the maturity method for AAM repair materials

The integration of maturity methods into AAM field practice serves as a critical bridge between laboratory mix design and on-site execution. In rapid pavement (or structural) repairs, decision-making regarding the reopening of pavements to traffic, the rapid removal of climbing formwork in core walls, or the early lifting of precast elements within a few hours cannot rely on standard 28-day laboratory cure times [5, 17]. Instead, modern performance-based scheduling demands real-time, *in-situ* strength verification.

Following the evidence in Section 3.4 that the exponential Arrhenius model provides superior early-age predictive accuracy for AAM systems over the linear Nurse-Saul approach, field deployment reveals a significant operational hurdle: the "crossover effect." This phenomenon is particularly prevalent in rapid-repair AAM mixtures where highly exothermic reactions promote the premature precipitation of dense reaction products. Such products form a non-uniform microstructure that restricts subsequent diffusion, ultimately truncating long-term strength development. For rapid pavement (or structural) repairs, this presents a critical dilemma between the mandate for immediate service against the requirement for long-term structural integrity. Maturity-based protocols, including ASTM C1074 and AASHTO T 413, offer a framework for monitoring strength under fluctuating temperatures; however, they often fail to account for the reduction in the ultimate strength threshold caused by excessive thermal acceleration. Effective management of the kinetics of highly reactive precursors is therefore as vital as the maturity monitoring itself to ensure that early reopening does not compromise the patch's service life.

To monitor these temperature-sensitive reactions under field conditions, the Modified Nurse-Saul (MNS) maturity function has been widely applied because it incorporates dynamic "acceleration" and "temperature-efficiency" factors, enabling more reliable strength estimation under non-isothermal curing histories [102, 103]. This aligns with emerging evidence that conventional formulations, particularly the linear Nurse-Saul approach, often fail to capture the synergistic effects of peak temperature, exposure duration, and subsequent cooling typical of AAM systems, as specimens with equivalent maturity indices can exhibit significantly different strength developments. To address this limitation, the "Weighted Maturity" concept assigns greater influence to early-age elevated temperatures, improving predictive accuracy by explicitly accounting for both peak temperature and exposure duration [99]. In addition, coupling maturity indices with sigmoidal strength development models, such as the Gompertz function, provides a realistic representation of nonlinear reaction kinetics and early-age strength gain. This approach shows strong predictive capability for slag-containing systems, particularly within the critical early strength range of 5–10 MPa required for rapid-repair operations [100].

Despite these mathematical advancements in maturity-based strength prediction, relying solely on embedded maturity sensors (e.g., thermocouples) introduces a spatial limitation in field applications. While maturity sensors provide continuous temporal monitoring of temperature history, their measurements remain strictly point-based and may therefore fail to capture strength variability across large pavement slabs or extensive repair patches [5]. To address this limitation, recent studies propose integrating the maturity method with spatial non-destructive testing techniques such as Ultrasonic Tomography (UST). As demonstrated by Kosar et al. [5], combining localized maturity indices with the rapid and portable imaging capability of UST enables a more comprehensive three-dimensional assessment of *in-situ* strength during the critical first 24 h, reducing the risk that undetected "cold spots" or poorly mixed zones prematurely trigger early-opening decisions.

Ultimately, the reliable implementation of AAM materials in rapid-repair scenarios depends on mixture-specific calibration and robust field monitoring strategies. Integrating the "Weighted Maturity" concept with sigmoidal strength-development models provides a promising framework to complement or calibrate the MNS approach, enabling more accurate prediction of early-age strength under temperature-sensitive curing conditions. In practice, embedding maturity sensors to track the thermal history of the repair patch, combined with periodic spatial verification using UST, allows engineers to determine when a repair element safely reaches operational thresholds; for example, lifting strengths of about 15 MPa at approximately 16 h for precast elements [17] or load-bearing capacities of ≥20 MPa within hours for pavement reopening [5]. Such performance-based monitoring reduces the risk of premature structural loading while also avoiding the

unnecessary traffic delays associated with overly conservative fixed-time curing schedules.

4.3 Identifying challenges and limitations

Despite the promising potential of AAMs for rapid pavement repair, their broader field deployment is constrained by a series of interconnected technical, operational, and systemic challenges. These limitations arise from fundamental material sensitivities, construction-related constraints, supply chain and economic uncertainties, and the limited availability of standardized testing frameworks and long-term field performance data.

Sensitivity to Activator Chemistry and Rheology: A major limitation in the field adoption of AAM-based repair materials is their strong sensitivity to activator chemistry, which directly governs reaction kinetics, rheological behavior, and setting characteristics. Small variations in alkalinity and Ms can significantly alter dissolution and polymerization processes, producing abrupt changes in viscosity, gelation rate, and workability. This narrow compositional tolerance is particularly challenging for slag-rich systems, which are typically required for rapid strength development but frequently exhibit limited workable windows due to poor workability and flash setting [24, 25, 41]. Consequently, the performance of AAM repair mixtures remains highly dependent on precise activator control, and even minor deviations during field batching can disrupt the balance between workability and early-age strength. Although one-part "just add water" systems improve handling safety and simplify logistics, they do not eliminate this intrinsic sensitivity. Instead, the critical parameters of alkali dosage and silicate availability are transferred into a dissolution-controlled activation framework that still requires careful calibration to maintain stable rheological behavior during practical repair operations.

Curing Sensitivity: Reliable strength development in pavement repair is strongly influenced by curing conditions, which are difficult to control under field environments. AAM systems exhibit pronounced temperature sensitivity. While slag-rich systems can generally develop strength at ambient conditions, Class F fly ash-based AAMs often experience delayed strength development without external heat, complicating early traffic reopening schedules. Chemical accelerators are frequently used to mitigate this limitation, but their effectiveness is constrained by a narrow operational window because excessive dosages may trigger rapid heat release, flash setting, and ultimately reduced long-term strength [58]. The strong coupling between temperature history and reaction progress also complicates the application of predictive tools such as the maturity method, which is widely used to determine safe traffic-opening times in pavement repair but remains more difficult to calibrate for AAMs than for OPC-based materials. Although active curing techniques such as electro-curing can accelerate early reactions, they also introduce an activation threshold beyond which excessive energy input may cause rapid moisture loss, microcracking, and strength regression rather than improvement [51].

Volumetric Stability: Regarding volumetric stability, dimensional consistency represents another critical limitation for repair applications in which the new material is restrained by the surrounding pavement. Slag-rich formulations, favored for their rapid strength development, are particularly susceptible to autogenous shrinkage and time-dependent deformation. Slag-based AAM mortars often exhibit high shrinkage due to their refined pore structure and associated capillary stresses [42, 63], while creep coefficients have been reported to exceed those of OPC-based systems [87, 88]. In constrained repair patches, this combination of shrinkage and creep can generate internal stresses that lead to early cracking and edge debonding during the hardening phase. Hybridizing slag with low-CaO precursors such as Class F fly ash can partially mitigate shrinkage [36, 63], but this strategy often introduces a trade-off with early-age strength gain, which is critical for rapid-repair strategies.

Supply Chain Stability and Economic Feasibility: Despite their well-documented mechanical and environmental advantages, the large-scale adoption of AAMs for rapid pavement repair remains constrained by economic feasibility and supply chain stability. Unlike OPC, which benefits from globally established production and distribution networks, AAMs rely on the consistent availability of specific industrial by-products and alkaline activators, creating logistical challenges for large-scale deployment [29, 78]. The supply of key precursors such as fly ash and slag is becoming increasingly uncertain due to structural changes in the coal power and steel industries, while variability in fineness, CaO content, and amorphous phase fraction can significantly influence reaction kinetics and strength development, complicating material qualification for field applications [9]. These challenges are further intensified by the geographic concentration of slag production near steel manufacturing hubs and the declining availability of high-quality fly ash in regions transitioning away from coal power. For rapid pavement repair operations that require reliable material availability and rapid mobilization, such supply uncertainties introduce transportation constraints and cost variability that can limit practical implementation. Moreover, although industrial by-products may reduce baseline material costs relative to OPC, these potential savings are often offset by the relatively high cost and limited availability of alkaline activators, which remain a major economic barrier to widespread adoption [9, 29, 78].

Lack of Standardized Testing and Long-Term Field Data: Finally, the broader adoption of AAM-based

repair materials is constrained by the lack of standardized testing protocols and limited long-term field performance data. Many durability assessment methods currently used in practice were originally developed for OPC-based materials and may yield inconsistent or misleading results when applied to AAMs due to differences in chemistry and pore structure. For example, conventional freeze-thaw testing protocols may not accurately represent the durability behavior of AAM systems [13], while field-scale validation of critical performance aspects such as fatigue under repetitive traffic loading remains extremely limited compared with the extensive datasets available for conventional concrete [62]. Surface-related issues such as efflorescence also remain practical concerns for exposed repair applications [28, 96]. Although short-term pilot projects, including the one-year campus road repair monitored by Chen et al. [27], have demonstrated encouraging performance, these observations remain insufficient when compared with the multi-decade service history of OPC. As highlighted by van Deventer et al. [104], the absence of multi-decade field data and the limited suitability of certain OPC-derived test methods for AAMs underscore the need for performance-based evaluation frameworks tailored to the unique chemistries and degradation mechanisms of AAM systems.

4.4 Implications for practice and future research

Building on the challenges identified in the previous section, the synthesis of current findings highlights several practical implications for the field deployment of AAMs in pavement repair, particularly in applications requiring rapid traffic reopening, operational efficiency, and improved sustainability. One of the most significant practical advancements enabling field implementation is the transition toward one-part formulations, which replace highly caustic liquid activators with safer solid activators such as sodium metasilicate pentahydrate and sodium hydroxide flakes. In these systems, the critical parameters of alkali dosage and silicate availability are governed by dissolution kinetics rather than liquid activator handling, improving safety and aligning AAM mixing procedures with conventional construction workflows [55, 70].

Successful implementation also depends on operational procedures tailored to specific repair techniques and supported by standardized frameworks for evaluating workability, thixotropy, and open time across patching, grouting, and shotcrete applications. High-early strength AAM grouts, for example, must balance fluidity with rapid-setting to ensure effective infiltration of aggregate gaps and the formation of a uniform microstructure [105]. Rheological parameters such as viscosity, wetting behavior, and air entrapment therefore play a critical role in defect formation during placement [72]. Similarly, shotcrete-based repairs require strict control of flow rate, spray angle, and nozzle distance to minimize rebound and ensure adequate material build-up in vertical or overhead sections, reflecting the pronounced rheological sensitivity of AAM mixtures [67]. At the material scale, optimized AAM mixtures can form dense, chemically integrated ITZs with existing substrates. The absence of free portlandite and the formation of zeolite-like phases enhance bond durability and load transfer under cyclic loading compared with OPC-based repair materials [4, 7, 101].

Beyond technical performance, the deployment of AAMs also provides significant sustainability benefits by valorizing industrial by-products such as slag and fly ash as reactive binders, thereby reducing clinker demand and lowering the carbon footprint of pavement rehabilitation. Additional residues, including red mud and flue gas desulfurization gypsum, have also been successfully incorporated into slag-based AAM systems, simultaneously reducing embodied carbon and immobilizing hazardous trace metals such as Pb, Cr, and As with high efficiency [52].

Looking forward, several research directions are essential to advance the field application of AAMs in rapid pavement repair. Key directions include refining one-part formulations to improve safety and constructability, establishing maturity-based monitoring frameworks tailored to ultra-early strength AAMs, and developing integrated strategies to mitigate the long-term durability risks associated with premature traffic loading.

Refinement of One-Part Formulations: Future research should prioritize optimized hybrid one-part AAM systems that combine CaO-rich precursors with aluminosilicate sources and are activated using moderately alkaline, silicate-bearing solid activators. Effective formulations are typically based on slag-dominant precursor blends supplemented with Class F fly ash or metakaolin, with optional silica-rich additives to enhance polymerization and refine pore structure. Na-based activators such as sodium metasilicate pentahydrate and sodium hydroxide flakes remain the most effective for CaO-rich systems due to their strong compatibility with slag chemistry. However, the transition to one-part AAMs shifts reaction control toward dissolution-driven activation, where the availability of soluble alkalis and silicates depends on the solubility kinetics of solid activators. This introduces a critical design constraint: incomplete dissolution delays strength development, while excessive alkalinity may accelerate setting and diminish workability. Consequently, practical mix design requires careful iterative adjustment of alkali dosage, silicate availability, and water-to-binder ratio to maintain a balance between early-age performance and adequate flowability during placement [106]. Since these parameters are intrinsically linked to the synergy between precursor and activator chemistry,

optimization increasingly relies on multi-factor statistical frameworks such as Response Surface Methodology (RSM), which can quantify their combined influence on key performance indicators including one-day compressive, flexural, and bond strengths [81]. When integrated with regression-based predictive modeling [107], these approaches enable reliable forecasting of performance and reaction kinetics, thereby reducing empirical trial-and-error and facilitating robust mix designs for rapid-repair applications.

Maturity Calibration for Ultra-Early Strength AAMs: Future studies should develop maturity-based monitoring frameworks specifically calibrated for AAM repair materials to support reliable "return-to-service" decisions in rapid pavement repair. Because AAMs exhibit different reaction mechanisms and temperature sensitivities compared with OPC, conventional maturity relationships must be reformulated using AAM-specific activation energies and strength-maturity correlations. Temperature-dependent maturity functions are particularly suitable, as they account for non-isothermal curing and the variable efficiency of temperature in driving reaction kinetics. Given the inherently non-linear and composition-dependent nature of AAM reactions, OPC-based models require systematic adjustment to ensure accurate strength prediction. Within this framework, the rate and cumulative heat release during the acceleration stage can serve as mechanistic proxies for strength development, linking thermokinetic evolution to structural build-up. Predictive capability can be further enhanced by coupling maturity indices with sigmoidal strength development models that capture the non-linear progression of strength gain. While maturity sensors track temporal reaction kinetics, they are limited to point-based data and may miss spatial inconsistencies. Integrating UPV and UST bridges this gap: UPV verifies material homogeneity through numerical velocity benchmarks, while UST provides high-resolution spatial imaging to detect localized internal defects or bonding failures. This combination ensures that the maturity-based strength predictions are physically validated by structural integrity and spatial uniformity across the entire repair patch.

Strategies to Mitigate Long-Term Degradation under Early Traffic Loading: Future research must address the compounding effects of shrinkage and durability degradation associated with premature traffic loading by adopting integrated material and structural design strategies. The development of strain-tolerant matrices with internal curing capability is an essential first step, as internal curing agents can sustain secondary hydration and mitigate autogenous shrinkage while flexible micro-fibers help absorb strain energy induced by early dynamic loading. Building on this foundation, mix designs may incorporate load-activated autonomous healing systems such as microencapsulated sodium silicate, which can release healing agents when triggered by traffic-induced vibration or shear stress [108]. These systems enable localized repair of micro-defects at early-ages when the aluminosilicate gel network remains vulnerable, thereby preventing crack propagation. To translate these material innovations into reliable field performance, it is also necessary to establish early-age chemo-mechanical fatigue modeling frameworks that simulate the combined effects of shrinkage and dynamic traffic loading. Standardized experimental protocols capable of simultaneously monitoring shrinkage and cyclic loading during ultra-early ages, typically within 6 to 24 h after placement, would generate the empirical data needed to develop probabilistic service-life models.

5 Conclusion

This systematic review synthesized the findings of 94 peer-reviewed studies to assess the suitability of AAM as a sustainable, rapid-hardening binder for concrete pavement repair. Additional supporting literature was incorporated to strengthen the methodological framework, clarify the material system, and examine the potential integration of AAMs with maturity-based strength prediction approaches.

Performance Evidence and Standard Compliance: The reviewed studies consistently demonstrate that optimized AAM mixtures outperform conventional Portland-based and alternative rapid-hardening repair materials, particularly in terms of early-age strength gain, bond performance, and durability. Optimized slag-containing mixtures frequently achieve compressive strengths exceeding 16–28 MPa within the first 6–8 h, satisfying the early-age strength requirements of ASTM C928 and meeting the structural repair criteria of BS EN 1504-3 "Class R4" at significantly earlier ages than conventional systems. AAM repair mortars also exhibit excellent interfacial bonding, with early tensile bond strengths well above the 2 MPa benchmark required for structural repair materials. In addition to mechanical performance, AAMs demonstrate superior durability characteristics, including substantially lower chloride transport, reduced water permeability, strong freeze-thaw resistance, and improved abrasion resistance compared with Portland-based materials.

Maturity-Based Practical Guidance: The integration of AAMs with maturity-based strength prediction offers a promising pathway for rapid-repair applications by linking temperature history to strength development and enabling more reliable "opening to traffic" decisions. However, the distinct and complex reaction kinetics of AAM binders require recalibration and validation of existing maturity functions. Furthermore, to address the point-based limitation of maturity sensors, integrating spatial non-destructive techniques is essential: while maturity monitoring

captures temporal kinetics, UPV and UST verify structural integrity and spatial uniformity, ensuring that repair zones are free from defects that temperature-based predictions alone may overlook.

Research Framework for the Future: Advancing AAM commercialization requires a multi-scale, lifecycle-oriented approach. At the micro-scale, mix designs must balance early-age performance, rheological stability, and shrinkage mitigation using optimization tools like RSM. Incorporate kinetic-based maturity frameworks at this stage allows for the translation of these optimized chemical properties into predictable hardening schedules across varying climatic conditions. At the meso-scale, integrating load-triggered autonomous self-healing systems and synthetic fibers is essential to counteract brittleness and dynamic traffic stresses. Finally, macro-scale research must establish decade-long field exposure sites to develop probabilistic service-life models and adapt standard testing protocols specifically for AAMs.

Acknowledgements

Not applicable.

Funding Statement

The authors received no specific funding for this study.

Author Contributions

The authors confirm contribution to the paper as follows: Conceptualization, Muhamad Aditya Pratama and Stefanus Adi Kristiawan; methodology, Muhamad Aditya Pratama and Stefanus Adi Kristiawan; software, Muhamad Aditya Pratama; validation, Florentina Pungky Pramesti and Stefanus Adi Kristiawan; formal analysis, Muhamad Aditya Pratama and Stefanus Adi Kristiawan; investigation, Muhamad Aditya Pratama; resources, Stefanus Adi Kristiawan; data curation, Muhamad Aditya Pratama and Florentina Pungky Pramesti; writing—original draft preparation, Muhamad Aditya Pratama; writing—review and editing, Stefanus Adi Kristiawan and Florentina Pungky Pramesti; visualization, Muhamad Aditya Pratama; supervision, Stefanus Adi Kristiawan and Florentina Pungky Pramesti. All authors reviewed and approved the final version of the manuscript.

Availability of Data and Materials

Not applicable.

Ethics Approval

Not applicable.

Conflicts of Interest

The authors declare no conflicts of interest.

REFERENCES

[1] Yeo SH, Mo KH, Hosen MA, Bin Mahmud H. Properties of cementitious repair materials for concrete pavement. Adv Mater Sci Eng. 2022;2022(1):3057801. doi:10.1155/2022/3057801.

[2] Zhao Z, Ma Q, Xu Q, Sun F. A review: fast repair technology of cement concrete pavement. E3S Web Conf. 2019;136:04053. doi:10.1051/e3sconf/201913604053.

[3] Tingle JS, Williams CE Jr, Carruth WD, Tibbetts CM. Materials and methods used for the expedient repair of concrete pavements. Eng Proc. 2023;36(1):43. doi:10.21079/11681/48710.

[4] Kryvenko P, Rudenko I, Sikora P, Sanytsky M, Konstantynovskyi O, Kropyvnytska T. Alkali-activated cements as sustainable materials for repairing building construction: a review. J Build Eng. 2024;90(6):109399. doi:10.1016/j.jobe.2024.109399.

[5] Kosar K, de Salles LS, Sharifi NP, Vandenbossche J, Khazanovich L. Onsite strength determination for early-opening decision making of high early strength concrete pavement. J Traffic Transp Eng Engl Ed. 2023;10(2):291–303. doi:10.1016/j.jtte.2021.12.005.

[6] Magee B, Woodward W, Tretsiakova-Mcnally S, Lemoine P. A preliminary investigation into geopolymer cement mortar's suitability for providing resilient highway solutions. In: Proceedings of the Sixth International Conference on the Durability of Concrete Structures; 2018 Jul 18–20; Leeds, UK.

[7] Laskar SM, Mozumder RA, Laskar AI. Behaviour of RC beam repaired using alkali activated slag-based agent under static and cyclic loading. Structures. 2021;31(6):761–8. doi:10.1016/j.istruc.2021.02.039.

[8] Pavel K, Oleg P, Hryhorii V, Serhii L. The development of alkali-activated cement mixtures for fast rehabilitation and strengthening of concrete structures. Procedia Eng. 2017;195:142–6. doi:10.1016/j.proeng.2017.04.536.

[9] Adnan, Anas M. Geopolymer concrete as a sustainable alternative to OPC. J Umm Al Qura Univ Eng Archit. 2025;16(4):1223–45. doi:10.1007/s43995-025-00155-8.

[10] Rudnicki T, Stałowski P. Fast-setting concrete for repairing cement concrete pavement. Materials. 2023;16(17):5909. doi:10.3390/ma16175909.

[11] Almonayea N, Garcia-Troncoso N, Xu B, Bompa DV. Probabilistic embodied carbon assessments for alkali-activated concrete materials. Sustainability. 2025;17(1):152. doi:10.3390/su17010152.

[12] Olayinka R, Jafari R, Fiset M. Shrinkage characteristics of geopolymer concrete: a comprehensive review. Materials. 2025;18(19):4528. doi:10.3390/ma18194528.

[13] Arbi K, Nedeljković M, Zuo Y, Ye G. A review on the durability of alkali-activated fly ash/slag systems: advances, issues, and perspectives. Ind Eng Chem Res. 2016;55(19):5439–53. doi:10.1021/acs.iecr.6b00559.

[14] Zhang H, Hu Z, Liu H, Li J, Jiang H. Mix-free, rapid-infiltration, and quick-setting road repair material based on MPC. J Phys Conf Ser. 2025;3112(1):012077. doi:10.1088/1742-6596/3112/1/012077.

[15] Detphan S, Hanjitsuwan S, Pangdaeng S, Phoo-ngernkham T, Damrongwiriyanupap N, Wongsa A, et al. Hybrid alkali-activated fly ash-Portland cement binders with modified polymer as patch repair. Constr Build Mater. 2024;436(1):136776. doi:10.1016/j.conbuildmat.2024.136776.

[16] Nandhini K, Karthikeyan J. The early-age prediction of concrete strength using maturity models: a review. J Build Pathol Rehabil. 2021;6(1):7. doi:10.1007/s41024-020-00102-1.

[17] Kanavaris F, Soutsos M, Chen JF. Enabling sustainable rapid construction with high volume GGBS concrete through elevated temperature curing and maturity testing. J Build Eng. 2023;63:105434. doi:10.1016/j.jobe.2022.105434.

[18] Provis JL, Bernal SA. Milestones in the analysis of alkali-activated binders. J Sustain Cem Based Mater. 2015;4(2):74–84. doi:10.1080/21650373.2014.958599.

[19] Bernal SA, Provis JL. Durability of alkali-activated materials: progress and perspectives. J Am Ceram Soc. 2014;97(4):997–1008. doi:10.1111/jace.12831.

[20] Fan J, Zhu H, Shi J, Li Z, Yang S. Influence of slag content on the bond strength, chloride penetration resistance, and interface phase evolution of concrete repaired with alkali activated slag/fly ash. Constr Build Mater. 2020;263(6):120639. doi:10.1016/j.conbuildmat.2020.120639.

[21] Shi S, Li H, Zhou Q, Zhang H, Basheer PAM, Bai Y. Alkali-activated fly ash cured with pulsed microwave and thermal oven: a comparison of reaction products, microstructure and compressive strength. Cem Concr Res. 2023;166(8):107104. doi:10.1016/j.cemconres.2023.107104.
[22] Abdellatief M, Alanazi H, Radwan MKH, Tahwia AM. Multiscale characterization at early ages of ultra-high performance geopolymer concrete. Polymers. 2022;14(24):5504. doi:10.3390/polym14245504.
[23] Sun B, Ye G, de Schutter G. A review: reaction mechanism and strength of slag and fly ash-based alkali-activated materials. Constr Build Mater. 2022;326(11):126843. doi:10.1016/j.conbuildmat.2022.126843.
[24] Huseien GF, Mirza J, Ismail M, Ghoshal SK, Ariffin MAM. Effect of metakaolin replaced granulated blast furnace slag on fresh and early strength properties of geopolymer mortar. Ain Shams Eng J. 2018;9(4):1557–66. doi:10.1016/j.asej.2016.11.011.
[25] Tran VA, Nguyen HA. Evaluation on comprehensive properties and bonding performance of practical slag-fly ash blending based alkali-activated material. J Build Eng. 2022;62(3):105350. doi:10.1016/j.jobe.2022.105350.
[26] Laskar SM, Talukdar S. Preparation and tests for workability, compressive and bond strength of ultra-fine slag based geopolymer as concrete repairing agent. Constr Build Mater. 2017;154(4):176–90. doi:10.1016/j.conbuildmat.2017.07.187.
[27] Chen K, Wu D, Yi M, Cai Q, Zhang Z. Mechanical and durability properties of metakaolin blended with slag geopolymer mortars used for pavement repair. Constr Build Mater. 2021;281(2):122566. doi:10.1016/j.conbuildmat.2021.122566.
[28] Abdayem J, Saba M, Tehrani FF, Absi J. Evaluating waste-based alkali activated materials as pavement quality concrete. Infrastructures. 2024;9(11): 190. doi:10.3390/infrastructures9110190.
[29] Amran M, Al-Fakih A, Chu SH, Fediuk R, Haruna S, Azevedo A, et al. Long-term durability properties of geopolymer concrete: an in-depth review. Case Stud Constr Mater. 2021;15:e00661. doi:10.1016/j.cscm.2021.e00661.
[30] Page MJ, McKenzie JE, Bossuyt PM, Boutron I, Hoffmann TC, Mulrow CD, et al. The PRISMA, 2020 statement: an updated guideline for reporting systematic reviews. BMJ. 2021;372:n71. doi:10.1136/bmj.n71.
[31] Liberati A, Altman DG, Tetzlaff J, Mulrow C, Gøtzsche PC, Ioannidis JPA, et al. The PRISMA statement for reporting systematic reviews and meta-analyses of studies that evaluate health care interventions: explanation and elaboration. BMJ. 2009;339:b2700. doi:10.1136/bmj.b2700.
[32] Methley AM, Campbell S, Chew-Graham C, McNally R, Cheraghi-Sohi S. PICO, PICOS and SPIDER: a comparison study of specificity and sensitivity in three search tools for qualitative systematic reviews. BMC Heal Serv Res. 2014;14(1):579. doi:10.1186/s12913-014-0579-0.
[33] Grant MJ, Booth A. A typology of reviews: an analysis of 14 review types and associated methodologies. Health Info Libraries J. 2009;26(2):91–108. doi:10.1111/j.1471-1842.2009.00848.x.
[34] Xiao Y, Watson M. Guidance on conducting a systematic literature review. J Plan Educ Res. 2019;39(1):93–112. doi:10.1177/0739456x17723971.
[35] Jang JG, Lee HK. Effect of fly ash characteristics on delayed high-strength development of geopolymers. Constr Build Mater. 2016;102(3):260–9. doi:10.1016/j.conbuildmat.2015.10.172.
[36] Aiken TA, Kwasny J, Zhou Z, McPolin D, Sha W. Factors affecting the drying shrinkage of alkali-activated slag/fly ash mortars. MRS Adv. 2023;8(22) :1266–72. doi:10.1557/s43580-023-00647-6.
[37] Alanazi H, Yang M, Zhang D, Gao ZJ. Early strength and durability of metakaolin-based geopolymer concrete. Mag Concr Res. 2017;69(1):46–54. doi:10.1680/jmacr.16.00118.
[38] Qader DN, Jamil AS, Bahrami A, Ali M, Arunachalam KP. A systematic review of metakaolin-based alkali-activated and geopolymer concrete: a step toward green concrete. Rev Adv Mater Sci. 2025;64(1):20240076. doi:10.1515/rams-2024-0076.
[39] He J, Bu X, Bai W, Zheng W, Gao Q, Wang Y. Preparation and properties of self-compacting alkali-activated slag repair mortar. Constr Build Mater. 2020;252:119034. doi:10.1016/j.conbuildmat.2020.119034.
[40] Ji X, Wang Z, Wang X, Zhao X, Zhang H, Zhang T. Microstructures and properties of alkali-activated slags with composite activator: effects of Na_2O equivalents. J Clean Prod. 2024;450(3):141754. doi:10.1016/j.jclepro.2024.141754.
[41] Musaddiq Laskar S, Talukdar S. Development of ultrafine slag-based geopolymer mortar for use as repairing mortar. J Mater Civ Eng. 2017;29(5): 04016292. doi:10.1061/(asce)mt.1943-5533.0001824.
[42] Hu NJ, Hüsken G, Gluth GJG, Kühne HC. The influence of activator composition on the strength, shrinkage and chloride migration resistance of alkali-activated slag mortars. Key Eng Mater. 2018;761(5):61–4. doi:10.4028/www.scientific.net/kem.761.61.
[43] Yang J, Sun Z, De Belie N, Snoeck D. Mitigating plastic shrinkage cracking in alkali-activated slag systems by internal curing with superabsorbent polymers. Cem Concr Compos. 2022;134(12):104784. doi:10.1016/j.cemconcomp.2022.104784.
[44] Lacante M, Delsaute B, Staquet S. Effect of solution-to-binder ratio and molarity on volume changes in slag binder activated by sodium hydroxide at early age. Materials. 2024;17(13):3308. doi:10.3390/ma17133308.
[45] Gomaa E, Sargon S, Kashosi C, Gheni A, ElGawady MA. Mechanical properties of high early strength class C fly ash-based alkali activated concrete. Transp Res Rec J Transp Res Board. 2020;2674(5):430–43. doi:10.1177/0361198120915892.
[46] Sun B, Ye G, De Schutter G. A review: the strength influence factors of slag and fly ash based alkali activated materials. In: Proceedings of the 4th International RILEM Conference on Microstructure Related Durability of Cementitious Composites (Microdurability2020); 2021 Apr 29–May 25; Online. p. 748–56.
[47] Sun B, Sun Y, Ye G, De Schutter G. A mix design methodology of slag and fly ash-based alkali-activated paste. Cem Concr Compos. 2022;126(11): 104368. doi:10.1016/j.cemconcomp.2021.104368.
[48] Sun Y, Liu Z, Ghorbani S, Ye G, De Schutter G. Fresh and hardened properties of alkali-activated slag concrete: the effect of fly ash as a supplementary precursor. J Clean Prod. 2022;370:133362. doi:10.1016/j.jclepro.2022.133362.
[49] Thakkar S, Chanda A, Rawat S. Early strength development of self-compacting geopolymer mortar using binary and tertiary blends of industrial wastes. Mater Today Proc. 2023;93(6):467–74. doi:10.1016/j.matpr.2023.08.089.
[50] Li J, Wang Z, Zhang T, Guo H, Zhao X, Wang X, et al. Enhancement of interfacial adhesion between alkali-activated repair materials and old cement substrates. Constr Build Mater. 2025;491:142738. doi:10.1016/j.conbuildmat.2025.142738.
[51] Balapanov B, Montayev S, Canpolat O, Aygun BF, Alkhabaze Y, Uysal M. Physical and mechanical evolution of ternary geopolymer mortars under various curing methods. Eng Technol Appl Sci Res. 2025;15(5):27406–20. doi:10.48084/etasr.12938.
[52] Jiang S, Wang X, Qi K, Wan X. Preparation and performance of a fast-hardening red mud based geopolymer repair mortar complexed with FGD. J Build Eng. 2025;108(2):112980. doi:10.1016/j.jobe.2025.112980.
[53] Ren B, Chai L, Liu Y, Ma R, Liu Z, Wang Y. Performance optimization design of high ductility cement-based alkali-activated municipal solid waste incineration fly ash composite for rapid repair material. Constr Build Mater. 2023;404:133301. doi:10.1016/j.conbuildmat.2023.133301.
[54] Hawa A, Tonnayopas D, Prachasaree W, Taneerananon P. Development and performance evaluation of very high early strength geopolymer for rapid road repair. Adv Mater Sci Eng. 2013;2013(1):764180. doi:10.1155/2013/764180.
[55] Kryvenko P, Rudenko I, Konstantynovskyi O, Kovalchuk A. Improvement of early strength of slag containing Portland cements. In: Hydraulic and civil engineering technology IX. Amsterdam, The Netherlands: IOS Press; 2024. doi:10.3233/atde241029.
[56] Yusslee E, Beskhyroun S. The potential of one-part alkali-activated materials (AAMs) as a concrete patch mortar. Sci Rep. 2022;12:15902. doi:10.1038/s41598-022-19830-0.
[57] Alanazi H, Yang M, Zhang D, Gao ZJ. Bond strength of PCC pavement repairs using metakaolin-based geopolymer mortar. Cem Concr Compos. 2016;65:75–82. doi:10.1016/j.cemconcomp.2015.10.009.
[58] Chen T, Ren B, Wang Z, Meng X, Ning Y, Lv Y. Effect of early strength agent on the hydration of geopolymer mortar at low temperatures. Case Stud Constr Mater. 2022;17:e01419. doi:10.1016/j.cscm.2022.e01419.
[59] Chen P, Li Y, Zhang J, Zhang Z, Wang D. Influence of interface agent and form on the bonding performance and impermeability of ordinary concrete repaired with alkali-activated slag cementitious material. J Build Eng. 2024;94:110043. doi:10.1016/j.jobe.2024.110043.
[60] Badkul A, Paswan R, Singh SK, Tegar JP. A comprehensive study on the performance of alkali activated fly ash/GGBFS geopolymer concrete pavement. Road Mater Pavement Des. 2022;23(8):1815–35. doi:10.1080/14680629.2021.1926311.
[61] Fan LF, Chen DK, Zhong WL. Effects of slag and alkaline solution contents on bonding strength of geopolymer-concrete composites. Constr Build Mater. 2023;406(3):133391. doi:10.1016/j.conbuildmat.2023.133391.
[62] Singh S, Sharma SK, Akbar MA. Evaluation of mechanical and durability properties along with flexural fatigue life of pavement quality geopolymer concrete. Innov Infrastruct Solut. 2023;9(1):4. doi:10.1007/s41062-023-01311-6.
[63] Luo L, Yao W, Liang G, Luo Y. Workability, autogenous shrinkage and microstructure of alkali-activated slag/fly ash slurries: effect of precursor composition and sodium silicate modulus. J Build Eng. 2023;73:106712. doi:10.1016/j.jobe.2023.106712.
[64] Ding YC, Cheng TW, Dai YS. Application of geopolymer paste for concrete repair. Struct Concr. 2017;18(4):561–70. doi:10.1002/suco.201600161.
[65] Mohamed OA. Effects of the curing regime, acid exposure, alkaline activator dosage, and precursor content on the strength development of mortar with alkali-activated slag and fly ash binder: a critical review. Polymers. 2023;15(5):1248. doi:10.3390/polym15051248.
[66] Shahedan NF, Hadibarata T, Al Bakri Abdullah MM, Jusoh MNH, Rahim SZA, Isia I, et al. Potential of fly ash geopolymer concrete as repairing and retrofitting solutions for marine infrastructure: a review. Case Stud Constr Mater. 2024;20:e03214. doi:10.1016/j.cscm.2024.e03214.
[67] Hwalla J, El-Hassan H, El-Mir A, Assaad JJ, El-Maaddawy T. Development of geopolymer and cement-based shotcrete mortar: impact of mix design parameters and spraying process. Constr Build Mater. 2024;449:138457. doi:10.1016/j.conbuildmat.2024.138457.
[68] Fan J, Zhang B. Repair of ordinary Portland cement concrete using alkali activated slag/fly ash: freeze-thaw resistance and pore size evolution of adhesive interface. Constr Build Mater. 2021;300:124334. doi:10.1016/j.conbuildmat.2021.124334.
[69] Yusslee E, Beskhyroun S. Performance evaluation of hybrid one-part alkali activated materials (AAMs) for concrete structural repair. Buildings. 2022;12(11):2025. doi:10.3390/buildings12112025.

[70] Dong T, Sun T, Xu F, Ouyang G, Wang H, Yang F, et al. Effect of solid sodium silicate on workability, hydration and strength of alkali-activated GGBS/fly ash paste. Coatings. 2023;13(4):696. doi:10.3390/coatings13040696.
[71] Huseien GF, Shah KW. Performance evaluation of alkali-activated mortars containing industrial wastes as surface repair materials. J Build Eng. 2020;30:101234. doi:10.1016/j.jobe.2020.101234.
[72] Lv B, Wang L, Zeng Q, Guo Z. An on-site test investigation on ultra-early-strength infiltration grouting geopolymer for rapid road repair. Acta Geotech. 2025;20(12):6641–61. doi:10.1007/s11440-025-02748-y.
[73] Lei M, Wang X, Meng H, Yan Z, Lin J, Wu Z. Study of fly ash-slag geopolymer mortar as a rapid strengthening agent for concrete structures. Constr Build Mater. 2023;394:132147. doi:10.1016/j.conbuildmat.2023.132147.
[74] He J, Zhu M, Sang G, Yu S, He J. Effect of PVA latex powder and PP fiber on property of self-compacting alkali-activated slag repair mortar. Constr Build Mater. 2023;408:133703. doi:10.1016/j.conbuildmat.2023.133703.
[75] Qian YC, Zhang L, Qiao WG, Li YZ, Wu Y, Zhao YR. Temperature and composition effects on fresh and hardened properties of slag-fly ash-silica fume alkali-activated grouting materials. Sci Rep. 2026;16:3384. doi:10.1038/s41598-025-33462-0.
[76] Dai X, Aydin S, Yardimci MY, Sun Y, De Schutter G. Effect of temperature on the fresh and hardened state properties of alkali-activated slag/fly ash mixtures. Mater Struct. 2023;56(5):107. doi:10.1617/s11527-023-02194-w.
[77] Duan P, Yan C, Luo W. A novel waterproof, fast setting and high early strength repair material derived from metakaolin geopolymer. Constr Build Mater. 2016;124:69–73. doi:10.1016/j.conbuildmat.2016.07.058.
[78] Kuang F, Long Z, Kuang D, Guo R, Sun J. Experimental study on preparation and properties of low content rubberized geopolymer mortar. Constr Build Mater. 2022;352:128980. doi:10.1016/j.conbuildmat.2022.128980.
[79] Zhang S, Wang C, Gao G. Study of the mechanical properties of alkali-activated solid waste cementitious materials at the interface. ACS Omega. 2022;7(30):26531–6. doi:10.1021/acsomega.2c02622.
[80] Cao D, Zhang B. Study on bonding strength, chloride penetration resistance, and microstructure of adhesive interface for the old concrete repaired by alkali activated materials. AIP Adv. 2023;13(5):055025. doi:10.1063/5.0151664.
[81] Ma Z, Dan H, Tan J, Li M, Li S. Optimization design of MK-GGBS based geopolymer repairing mortar based on response surface methodology. Materials. 2023;16(5):1889. doi:10.3390/ma16051889.
[82] Bao K, Zhang G, Lv J, Li J, Chen Z, Yuan J. Bonding performance and microstructural mechanism between rapid repair materials and old concrete pavement. Buildings. 2024;14(7):2156. doi:10.3390/buildings14072156.
[83] Zanotti C, Borges PHR, Bhutta A, Banthia N. Bond strength between concrete substrate and metakaolin geopolymer repair mortar: effect of curing regime and PVA fiber reinforcement. Cem Concr Compos. 2017;80:307–16. doi:10.1016/j.cemconcomp.2016.12.014.
[84] Phoo-ngernkham T, Hanjitsuwan S, Li LY, Damrongwiriyanupap N, Chindaprasirt P. Adhesion characterisation of Portland cement concrete and alkali-activated binders. Adv Cem Res. 2019;31(2):69–79. doi:10.1680/jadcr.17.00122.
[85] Peter C, Karthi L. Experimental investigations on fibre reinforced geopolymer concrete as repair material for pavements. Sust Agric Food Env Res. 2023;12(1):1–16. doi:10.7770/safer-v12n1-art2779.
[86] Guo S, Lu Y, Wan X, Wu F, Zhao T, Shen C. Preparation, characterization of highly dispersed reduced graphene oxide/epoxy resin and its application in alkali-activated slag composites. Cem Concr Compos. 2020;105:103424. doi:10.1016/j.cemconcomp.2019.103424.
[87] Hojati M, Rajabipour F, Radlińska A. Creep of alkali-activated cement mixtures. Case Stud Constr Mater. 2022;16:e00954. doi:10.1016/j.cscm.2022.e00954.
[88] Caron R, Patel RA, Dehn F. Experimental study on basic and drying creep for an alkali-activated slag concrete and comparison with existing creep models. Struct Concr. 2023;24(5):6405–20. doi:10.1002/suco.202300134.
[89] Ascensão G, Marchi M, Segata M, Faleschini F, Pontikes Y. Increasing the dimensional stability of CaO-FeOx-Al_2O_3-SiO_2 alkali-activated materials: on the swelling potential of calcium oxide-rich admixtures. Detritus. 2019;8:91–100. doi:10.31025/2611-4135/2019.13880.
[90] Kryvenko PV, Vozniuk GV, Goncharova AM, Kavalerova ES. Shrinkage-compensating alkali activated slag cement mortars for crack repair and joint grouting in concretes. Adv Mater Res. 2014;923:134–7. doi:10.4028/www.scientific.net/amr.923.134.
[91] Feng B, Liu J. Durability of repair metakaolin geopolymeric cement under different factors. Processes. 2022;10(9):1818. doi:10.3390/pr10091818.
[92] Jahandari S, Tao Z, Rahmani A, Alim MA. Durability of one-part geopolymer concrete in aggressive environments. Constr Build Mater. 2025;490(5):142510. doi:10.1016/j.conbuildmat.2025.142510.
[93] Gluth GJG, Hlaváček P, Reinemann S, Ebell G, Mietz J. Leaching, carbonation and chloride ingress in reinforced alkali-activated fly ash mortars. MATEC Web Conf. 2018;199:02025. doi:10.1051/matecconf/201819902025.
[94] Sitarz M, Hager I, Choińska M. Evolution of mechanical properties with time of fly-ash-based geopolymer mortars under the effect of granulated ground blast furnace slag addition. Energies. 2020;13(5):1135. doi:10.3390/en13051135.
[95] Ghafoori N, Najimi M. Properties of alkali-activated fly ash/slag repair mortars. In: Proceedings of the 5th International Conference on Concrete Repair; 2014 Sep 1–3; Belfast, UK. p. 77–81. doi:10.1201/b17394-13.
[96] Zhang M, Zhao Y, Chen B. Efflorescence mitigation in fly ash/slag-based geopolymers: the role of precursor composition and proportions, and admixtures. Constr Build Mater. 2024;438(5):137216. doi:10.1016/j.conbuildmat.2024.137216.
[97] Ferreira L, Branco FG, Costa HSS, Júlio E, Maranha P. Characterization of alkali-activated binders using the maturity method. Constr Build Mater. 2015;95:337–44. doi:10.1016/j.conbuildmat.2015.07.068.
[98] Abdulmajid RR, Bzeni DK, Abed FH, Hamada HM. Feasibility of the maturity concept for strength prediction in geopolymer based materials. J Compos Sci. 2025;9(7):329. doi:10.3390/jcs9070329.
[99] Shin S, Goh G, Lee C. Predictions of compressive strength of GPC blended with GGBFS developed at varying temperatures. Constr Build Mater. 2019;206:1–9. doi:10.1016/j.conbuildmat.2019.01.181.
[100] Kim HS, Lee HS. Effect of GGBFS content and curing temperature on early-age strength and maturity-based modeling of concrete. Materials. 2025;18(19):4525. doi:10.3390/ma18194525.
[101] Vaičiukynienė D, Liudvinavičiūtė A, Bistrickaitė R, Boiko O, Vaičiukynas V. Alkali-activated slag repair mortar for old reinforced concrete structures based on ordinary Portland cement. Materials. 2025;18(10):2272. doi:10.3390/ma18102272.
[102] Soutsos M, Kanavaris F. The modified Nurse-Saul (MNS) maturity function for improved strength estimates at elevated curing temperatures. Case Stud Constr Mater. 2018;9(6):e00206. doi:10.1016/j.cscm.2018.e00206.
[103] Soutsos M, Kanavaris F. Applicability of the Modified Nurse-Saul (MNS) maturity function for estimating the effect of temperature on the compressive strength of GGBS concretes. Constr Build Mater. 2023;381(6):131250. doi:10.1016/j.conbuildmat.2023.131250.
[104] van Deventer JSJ, San Nicolas R, Ismail I, Bernal SA, Brice DG, Provis JL. Microstructure and durability of alkali-activated materials as key parameters for standardization. J Sustain Cem Based Mater. 2015;4(2):116–28. doi:10.1080/21650373.2014.979265.
[105] Liu J, Feng H, Zhang Y, Zheng K. Performance investigation of geopolymer grouting material with varied mix proportions. Sustainability. 2022;14(20):13046. doi:10.3390/su142013046.
[106] Liu S, Hao Y. Designing sprayable EGC from constructability to mechanical performance. J Build Eng. 2025;111:113509. doi:10.1016/j.jobe.2025.113509.
[107] Peng X, Zhuang Z, Yang Q. Predictive modeling of compressive strength for concrete at super early age. Materials. 2022;15(14):4914. doi:10.3390/ma15144914.
[108] Yin K, Luo Z, Liu X, Pan H, Zhi T, Feng H, et al. Preparation and application of Na_2SiO_3@EC microcapsules for self-healing alkali-activated slag. Constr Build Mater. 2023;400:132651. doi:10.1016/j.conbuildmat.2023.132651.